

Article

Comparative Studies on Batteries for the Electrochemical Energy Storage in the Delivery Vehicle

Piotr Szewczyk  and Andrzej Lebkowski * 

Department of Ship Automation, Gdynia Maritime University, Morska 83 Str., 81-225 Gdynia, Poland

* Correspondence: a.lebkowski@we.umg.edu.pl

Abstract: The publication presents a proposal of methodology for the evaluation of electric vehicle energy storage, based on examples of three types of batteries. Energy stores are evaluated in different categories such as cost, reliability, total range, energy density, battery life, weight, dependency on ambient temperature, and requirements of battery conditioning system. The performance of the battery systems were analyzed on exemplary 4×4 vehicle with 4 independent drives systems composed of inverters and synchronous in-wheel motors. The studies showed that the best results were obtained for energy storage built on LFP prismatic batteries, and the lowest ranking was given to energy storage built on cylindrical NMC batteries. The studies present the method of aggregation of optimization criteria as a valuable methodology for assessing design requirements and the risk of traction batteries in electric vehicles.

Keywords: battery energy storage system; electric vehicle; battery electric vehicle; in-wheel motor; wheel hub motor; reliability engineering



Citation: Szewczyk, P.; Lebkowski, A. Comparative Studies on Batteries for the Electrochemical Energy Storage in the Delivery Vehicle. *Energies* **2022**, *15*, 9613. <https://doi.org/10.3390/en15249613>

Academic Editor: Xianke Lin

Received: 24 November 2022

Accepted: 15 December 2022

Published: 18 December 2022

Publisher's Note: MDPI stays neutral with regard to jurisdictional claims in published maps and institutional affiliations.



Copyright: © 2022 by the authors. Licensee MDPI, Basel, Switzerland. This article is an open access article distributed under the terms and conditions of the Creative Commons Attribution (CC BY) license (<https://creativecommons.org/licenses/by/4.0/>).

1. Introduction

Reduction of CO₂ emissions and attempts to influence global warming have been two of the main goals of the economies of developed countries for many years. One of the main factors significantly affecting the emission of greenhouse gases is transport, which is why developed countries, have adopted strategies for the sustainable development of transport, which specify in detail the required actions in this direction in time intervals. The transport policy of the European Union has developed long-term plans, which, among other things, assume a 60% reduction in CO₂ emissions from the transport sector by 2050 compared to the 1990 level [1–5]. One of them is to increase the role of electric vehicles in road transport and to adapt the appropriate infrastructure for the development of electromobility.

The development of electric vehicle technology is closely related to the methods of energy storage. In modern electric vehicles, the most popular method of energy storage is in electrochemical lithium-ion batteries, however, their remaining problem is how to accurately determine the degree of battery life and the actual capacity available for energy. Accurate determination of these parameters is critical due to the predictability of operation and the estimated range of the vehicle.

The basic parameters characterizing lithium-ion batteries are: capacity, nominal voltage, energy and power density, continuous and peak current carrying capacity, maximum charging current, and operating temperature. The key parameters necessary for estimation during the life of the battery are the state of charge (SOC) of the battery in relation to the nominal capacity, as well as the life of the cell, which determines the state of health (SOH) of the battery. When assessing these values, additional quantities important to understand the condition of Li-ion batteries are: Depth of Discharge (DOD), Depth of Charge (DOC), Open Circuit Voltage (OCV), and Internal Resistance (IR).

Lithium-ion batteries are characterized by a high non-linearity of the discharge voltage characteristics as a function of the state of charge, and are also dependent on temperature

changes [6]. Therefore, their modeling is a challenge, especially at operating points where it is impossible to carry out a continuous measurement.

The SOC parameter is one of the main attributes of the cell and is defined as the ratio of the current capacity during the measurement to the nominal value. In the case of energy storage in an electric vehicle, this parameter is critical for the estimation of the vehicle range. The most accurate methods of measurement SOC are used only in the laboratory or in the post-production process, and the main purpose is to define dependencies of battery critical parameters in full operational range. One of the basic methods of measuring SOC is the open-circuit discharge test (SOC-OCV) that allows to determination of the SOC-OCV (voltage to SOC) characteristics. Another laboratory method used for assessing the state of charge and battery health is the internal resistance measurement. This method is based on the observation that during the operation of a lithium-ion battery, material degradation processes occur, which cause an increase in the internal resistance of the cell, which causes a decrease in its efficiency [7–9].

The most common method of estimating SOC in operating conditions is the so-called load-counting Coulomb method [10]. The advantage of this method is the ability to perform the measurement without the need to disconnect the load at the battery terminals. In practice, counting the total charge taken by the energy storage is done by measuring the currents flowing in and out of the battery, and then their values are integrated and compared with a predetermined mathematical model.

$$SOC = SOC(t_0) + \frac{1}{C_{rated}} \int_{t_0}^{t_0+\tau} (I_b - I_{loss}) dt \quad (1)$$

where: $SOC(t_0)$ is the initial state of charge, C_{rated} is the rated capacity of the battery, I_b is the current flowing through the cell, and I_{loss} is the loss current [11].

There are many other methods in the literature, such as those that use fuzzy logic [10], neural networks [7,12], the concept of the Kalman filter [13–15], adaptive methods [16], considering temperature and ageing [17] or various types of learning algorithms [18].

The state of health of the battery is another parameter that is very important in energy storage research. Modeling of SOH requires the development of an aging model that is based on time-consuming accelerating testing in various operating conditions [19]. Accelerated aging studies require finding the factors that most influence the change of critical battery parameters and estimating the accelerating factor (AF), which refers to the operation in real operating conditions.

The main factors influencing the aging process in batteries are temperature, the current flowing through the cell, and electric field strength in the electrolyte measured as the voltage at the terminals [19]. These three measurable parameters during operation are used to estimate the state of energy storage conditions in the analyzed environment [20]. Important parameters affecting SOH during the operation of the energy storage are the DOC and DOD in a given cycle. Based on these parameters, the percentage of energy storage consumption is estimated by comparing the measured values with the previously developed aging model of the tested energy storage. The example of the methods of determining the SOH is based on dependencies on changes in internal resistance, as discussed in [21,22], or the method of electrochemical impedance spectroscopy (analysis of the Nyquist characteristic) [19]. Adaptive methods using Kalman filters [13], fuzzy logic algorithms [10], or neural networks [23] are increasingly common in the literature. They allow for a more accurate estimation of the state of charge by analyzing the data of electrochemical processes characterized by high non-linearity [22,24,25]. Some of the more advanced methods analyze the rate of DOC and DOD and justify the effect of microcycles in the SOH algorithm, which gives a much more accurate picture of energy storage consumption. This is an important factor in the case of e.g., regenerative braking where the magazine is topped up to a limited extent at short intervals [19].

The state of wear of a battery cell at the rated temperature T_n and rated current I_n is easiest to present using the relationship [19]:

$$SOH = \frac{C(I_n, T_n)}{C_{BOL}(I_n, T_n)} \quad (2)$$

where: SOH is the State of Health) (%); C is the current electric capacity of the cell, and C_{BOL} is the electric capacity of the new cell.

One of the main criteria for the division of lithium-ion cells used in mobile energy storage is the chemical composition used in the construction of the battery cell. Due to the material used to build the cathode, the most commonly used cells in electric vehicles are lithium nickel aluminum (NCA), lithium manganese (LMO), lithium iron phosphate, and increasingly used nickel manganese cobalt (NMC) cells [26].

The purpose of this publication is to analyze the selection of electrochemical energy storage cells for a delivery vehicle with an electric drive. Among the many currently used types of electrochemical cells in their typical packaging, three types of cells were analyzed: LiFeYPO₄—LFP prismatic (WB-LYP100AHA cells were selected for testing), LiNiMnCoO₂—NMC cylindrical (Samsung 18650 Li-ion 3000 mAh INR18650-30Q), and LiNiMnCoO₂—NMC pouch (LG E76 cells were selected for testing).

For the presented types of cells, on the basis of tests using a real electric vehicle, the energy demand was estimated in various operating conditions, including changing environmental conditions, mainly temperature, and road conditions including changes in speed and slope. The profitability of using a given type of cells was analyzed, taking into account the charging levels of the energy storage, temperature conditions during operation, as well as the reliability of the storage structure, depending on the components used and the configuration of the cells in the storage. Based on the developed models, the service life (SOH) and the cost-effectiveness of the choice of a given electrochemical cell technology were estimated.

2. Materials and Methods

2.1. Electric Vehicle Range

One of the main operating parameters of the vehicle is its range, defined as the distance traveled by the vehicle with full use of energy storage. In the case of an electric vehicle, this applies to the full use of energy stored in the batteries under certain driving and speed conditions [27]. The range of the vehicle depends on design factors, operating conditions, and resistance to motion [28]. Below are the most important dependencies that are taken into account in the simulation of an electric vehicle.

All forces included in the developed model can be represented by the following equation:

$$F_F = F_{RR} + F_{air} + F_s + F_I + F_{IWD} \quad (3)$$

Rolling resistance force F_{RR} :

$$F_{RR} = \mu \cdot m_{tot} \cdot g \quad (4)$$

where: μ is the coefficient of friction, m_{tot} is the mass of the vehicle with load and energy storage, m_{ev} is the mass of the vehicle without the energy storage, m_{es} is the mass of the energy storage, and m_{load} is the mass of the load.

$$m_{tot} = m_{ev} + m_{es} + m_{load} \quad (5)$$

The F_{air} drag force is calculated from the following relationship:

$$F_{air} = \frac{1}{2} \rho_p \cdot C_x \cdot A_{front} \cdot V^2 \quad (6)$$

where: ρ_p is the air density (constant 1205 kg/m^3), C_x is the drag coefficient, V is the vehicle speed, and A_{front} is the frontal area of the vehicle.

The sliding force F_I is described by the following equation:

$$F_S = m_{tot} \cdot g \cdot \sin(\alpha) \quad (7)$$

Driving resistance dependent on acceleration or braking is calculated from the relationship between the total weight of the vehicle and acceleration/braking a :

$$F_I = m_{tot} \cdot a \quad (8)$$

Losses resulting from the transmission of drive in a 4×4 vehicle powered by an electric motor placed in the wheel depend on the torque generated by the T_{IWD} motor at a given radius of the vehicle wheel r :

$$F_{IWD} = \frac{T_{IWD}}{r} \quad (9)$$

2.2. Energy Storage System Configuration

As mentioned above, three types of cells were adopted to analyze the energy storage of the delivery vehicle: LFP prismatic, NMC 18,650 cylindrical, and NMC pouch.

The first type of cells, i.e., lithium iron phosphate LFP (LiFeYPO_4) cells, have a significantly lower energy density of $90\text{--}120 \text{ Wh/kg}$ and a lower nominal voltage of 3.2 V compared to the technology mentioned above. In addition, they have a higher self-discharge rate. On the other hand, these cells enable operation in a wide range of temperatures, high charging (5 C), and discharging (30 C) currents, and offer a long service life of more than 5000 cycles. In addition, among lithium-ion technologies, these cells are considered safe due to high thermal and chemical stability, resistance to emergency conditions, i.e., deep discharge, overcharge, short circuit, and high resistance to mechanical damage. For this reason, it is a technology that is particularly used for applications in harsh environmental conditions and in particular in the absence of thermal conditioning systems. Cells with chemistry of this type are most often implemented in the form of cuboids. The numerous advantages of LiFeYPO_4 cells have also contributed to a significant share in the field of electromobility. Figure 1 shows the capacity characteristics for the WB-LYP160Ah cells as a function of the number of cycles for the adopted operating ranges of $0\text{--}100\%$, $10\text{--}90\%$, $20\text{--}80\%$, and $30\text{--}70\%$ [29].

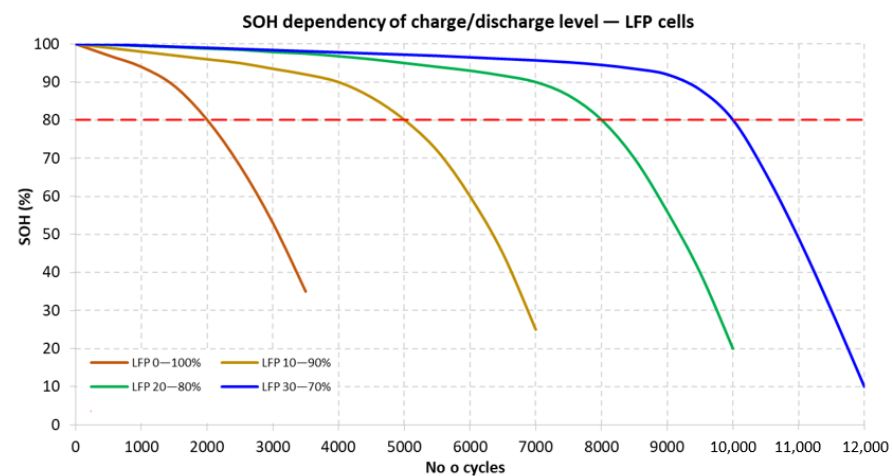


Figure 1. Loss of capacity of Winston WB-LYP160Aha cells as a function of the number of cycles for different operating ranges.

Lithium-nickel-manganese-cobalt NMC cells (LiNiMnCoO_2) are characterized by an energy density of $160\text{--}230 \text{ Wh/kg}$, a nominal voltage of 3.6 V , and average values

of charging current (0.7–1 C) and discharging (1–3 C). These cells are most often in the form of flat aluminum bags, which means that they are called “pouch” cells. The biggest disadvantage of this technology is the small number of cell cycles, an average of 500–1000. As of today, they constitute a dominant part of the battery market for electric and hybrid cars by Nissan, BMW, Renault, Kia, and many others. Figure 2 shows the capacity characteristics for INR18650-30Q cells as a function of the number of cycles for the adopted operating ranges of 0–100%, 10–90%, 20–80%, and 30–70%.

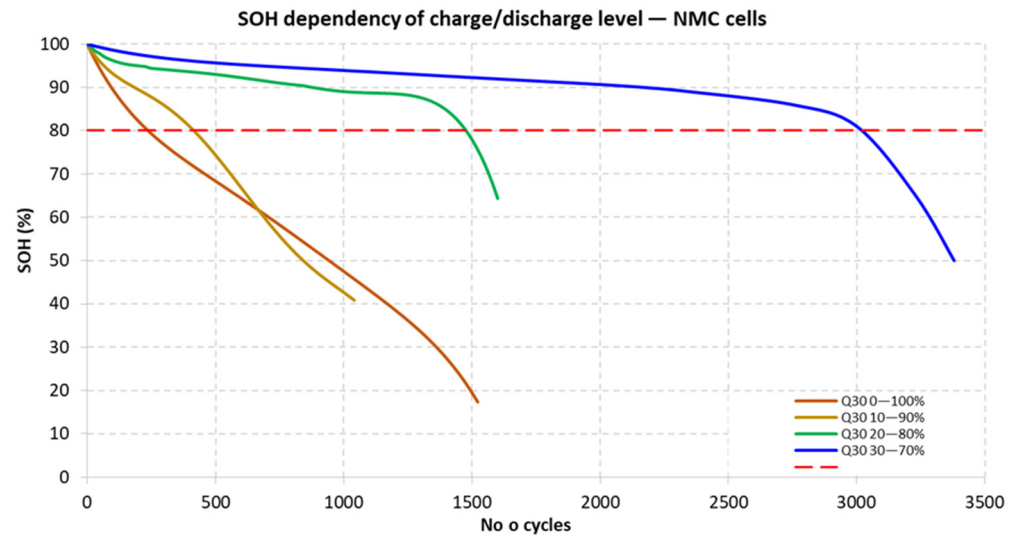


Figure 2. Loss of capacity of NMC Samsung INR18650–30Q cells as a function of the number of cycles for various operating ranges.

Figure 3 shows the dependence of the internal resistance of the analyzed cells depending on their temperature.

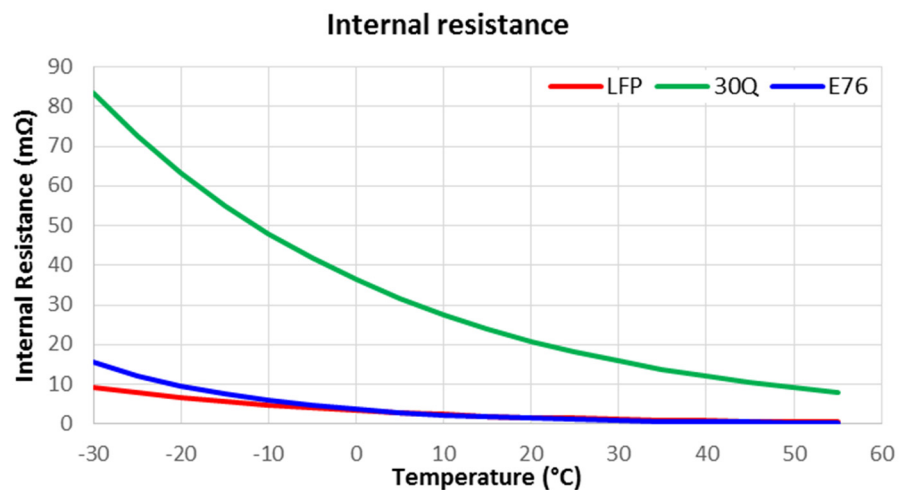


Figure 3. Dependence of internal resistance versus temperature for LFP—WB-LYP160, NMC—30Q, NMC—E76 (at load of 1C).

The tests were carried out on a 4×4 vehicle consisting of four sets of drives with motors placed in the wheel hub (Figure 4). The inverter is located not far from the engine on board the vehicle. Similar to the inverter, the energy storage is located centrally in the vehicle frame. Thanks to the modular design of the energy storage, it was possible to build replaceable cassettes containing different types of cell chemistry and corresponding connection configurations, the details of which are presented in Table 1.

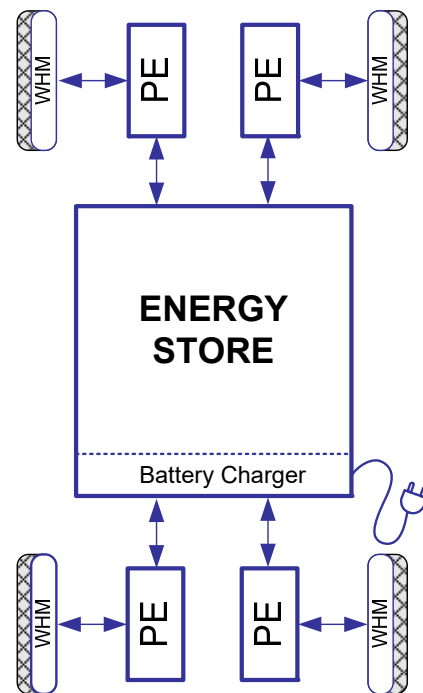


Figure 4. Configuration of the electric drive system with four electric motors installed in the wheels of the vehicle and inverter on board the vehicle. PE—Power Electronics (Inverter), WHM—Wheel Hub Motor.

Table 1. Energy storage parameters.

| Energy Store | ES Type 1 | ES Type 2 | ES Type 3 |
|---------------------------|---------------|--------------|-----------|
| Cell type | LFP-WB-LYP160 | INR18650-30Q | LG E76 |
| Cell shape | Prismatic | Cylindrical | Pouch |
| Cell chemistry | LFP | NMC | NMC |
| Store configuration (s-p) | 126-1 | 112-54 | 118-2 |
| Number of cells | 126 | 6048 | 236 |
| Nominal voltage (V) | 403.2 | 403.2 | 424.8 |
| Nominal capacity (Wh) | 64,512 | 65,318 | 64,570 |
| Mass (kg) | 789 | 314 | 293 |

2.3. Reliability Engineering

Reliability is an important non-functional parameter of any road vehicle and its quantitative estimation at the design stage is a major challenge. For this purpose, it is necessary to carry out many tests and analyses, identify critical system elements, and assess the risk and failure rate during operation. In a vehicle powered by electricity, an additional element that has a significant impact on reliability is energy storage. In contrast to internal combustion vehicles, in which the energy is stored in the fuel tank, electrochemical energy storage devices are much more complex devices and have a higher failure rate [30,31].

System reliability is defined as the probability that a given component or system will be able to perform the required functions under given conditions for a certain period of time and mathematically as R :

$$R(t) = e^{-\lambda t} \quad (10)$$

where: R is Reliability and λ is failure rate (1/year).

The probability of failure-free operation of the entire system depends on the product of the reliability of each component of the energy storage. This can be written by the formula below:

$$R_S = R_1 \cdot R_2 \cdot \dots \cdot R_n \quad (11)$$

The Reliability Block Diagram (RBD) model represents the dependence of the basic components of the energy storage in order to assess their impact on the reliability of the entire system, where R_S is the reliability of the entire system, and R_n designates the reliability of a single component in the system. Figure 5 shows a simplified RBD used for the estimation of the reliability of analyzed energy storage.

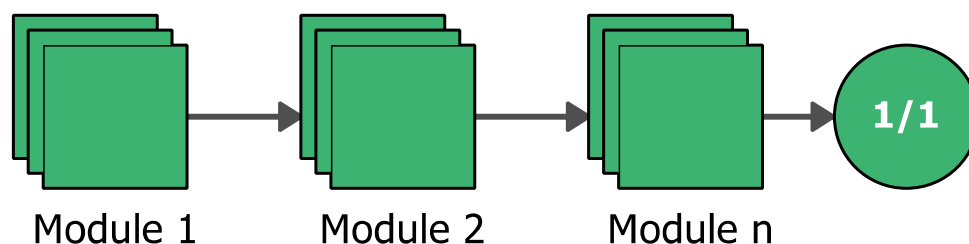


Figure 5. Reliability block diagram of vehicle energy storage (all types).

In the analyzed energy storage systems, a serial system was assumed, which accepts the share of failure of a single system component in the failure rate of the entire system. The model assumes that failure-free operation of all components of the energy storage is required for the full functionality of the energy storage. This assumption is a certain simplification, because in most cases a failure of a single cell does not cause a complete lack of power supply to the electric drive, but it causes more or less noticeable limitations, e.g., in power or range, and may also contribute to increasing the safety of use.

Table 2 presents the assumptions and results of the RBD analysis of the considered energy storage configurations.

Table 2. Reliability analysis of different types of ES Types results.

| Energy Storage Type | Config. (s-p) | Number of Cells | Nominal Voltage (V) | Statistical Distribution | Single Cell Reliability R_{bat} | Mission Time (y) | ES System Reliability | Failure Rate (1/y) |
|---------------------|---------------|-----------------|---------------------|--------------------------|-----------------------------------|------------------|-----------------------|--------------------|
| Type 1 | 126s1p | 126 | 403.2 | Exponential | 0.995 | 10 | 0.532592 | 0.006 |
| Type 2 | 112s54p | 6048 | 403.2 | Exponential | 0.995 | 10 | $7.36 \cdot 10^{-14}$ | 3.024 |
| Type 3 | 118s2p | 236 | 424.8 | Exponential | 0.995 | 10 | 0.307279 | 0.118 |

The analysis assumed the reliability of a single battery cell $R_{bat} = 0.995$ (99.5%), the mission time $y = 10$ years [31], and a one-parameter exponential distribution was assumed as the model type. The analysis of the obtained results (Figure 6) shows that the Type 1 (LFP prismatic) energy storage has the best parameters in terms of reliability, with a reliability of 0.5325 under the above-mentioned assumptions, and the estimated failure rate is 0.006 per year. Type 3 energy storage (NMC pouch) with NMC chemistry has a reliability of 0.3072 and an expected failure rate of 0.118 failures/year. The worst in terms of reliability is the Type 2 energy storage, built of cylindrical cells, showing a very high statistical failure rate of over three failures per year. This is justified by the very large number of components (6048 pcs) included in this system. It should be clarified here that in the case of energy storage built on cylindrical cells, a failure of one cell does not mean a critical failure of the entire system, but it is registered by the diagnostic system and signals the problem at the next service action.

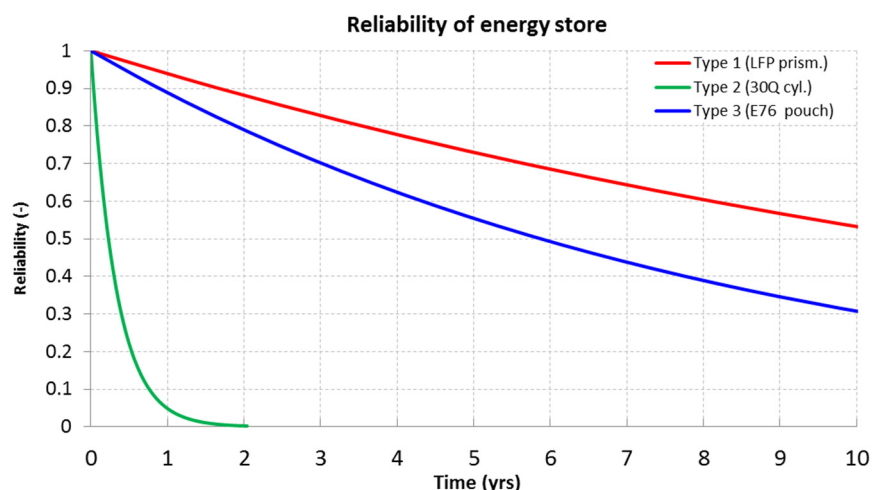


Figure 6. Reliability of different energy storage systems: Type 1: LFP—prismatic, Type 2: 30Q—cylindrical, Type 3: E76—pouch.

2.4. Test Cycles

Three test procedures WLTP, WLTP-90, and City Flat Road were selected for the study. The laboratory test WLTP (Worldwide Harmonized Light Vehicle Test Procedure, WLTP) [32,33] is a global standard that allows the comparison of exhaust emissions and energy consumption of light vehicles in different regions of the world. The WLTP procedure for each group of vehicles (class) determines four driving sections with different speeds: low, medium, high, and very high. In each of these parts, the driving, acceleration, braking, and standstill phases are separated.

The WLTP test cycle (World Harmonized Light Vehicle Test Procedure) reproduces the conditions of traffic intensity prevailing both in cities and on the motorway. This is a test cycle that, from 1 September 2017, replaced the previously used NEDC schedule. From 1 September 2019, the WLTP cycle is the basic cycle for testing the energy consumption of all newly manufactured cars. This cycle is intended for electric vehicles, motor vehicles, and light commercial vehicles. The WLTP test schedule was developed in 2015 by automotive experts mainly from the European Union, Japan, and India, in accordance with the guidelines of the UNECE World Forum for Harmonization of Vehicle Regulations. In 2017, the test cycle was modified for individual test classes [33].

In accordance with the provisions contained in Sub-Annexes 1 and 8 of Commission Regulation (EU) 2017/1151 [33], electric vehicles (PEV) are class 3 vehicles, and if their speed does not exceed 120 km/h—class 3a. According to Sub-Annex 1, energy consumption tests for this type of vehicle should be carried out on the basis of the WLTP test cycles: the Low₃(A1/7) phase, the Medium₃₋₁(A1/8) phase, the High₃₋₁(A1/10) phase, Extra High₃(A1/12), and the characteristics of which are shown in Figure 7.

For the WLTP test cycle, the average vehicle speed is 46.39 km/h, and the maximum speed is 131.3 km/h. The duration of the test is 1800 s and the length of the test route is 23.19 km [33].

The WLTP test procedure allows vehicles with a design-limited maximum speed to be tested below the maximum cycle speed of a given class by carrying out a modified test. According to the procedure, once the vehicle reaches its maximum speed, it should be maintained at this speed. In addition, the period of operation at this speed should be increased by the time that the distance traveled during each test segment is equal to the distance traveled during the unmodified test [33]. On this basis, most electric drive systems of delivery vehicles are tested, where the limit speed is often 90 km/h. In this situation, the test procedure is designated as WLTP-90 (Figure 8).

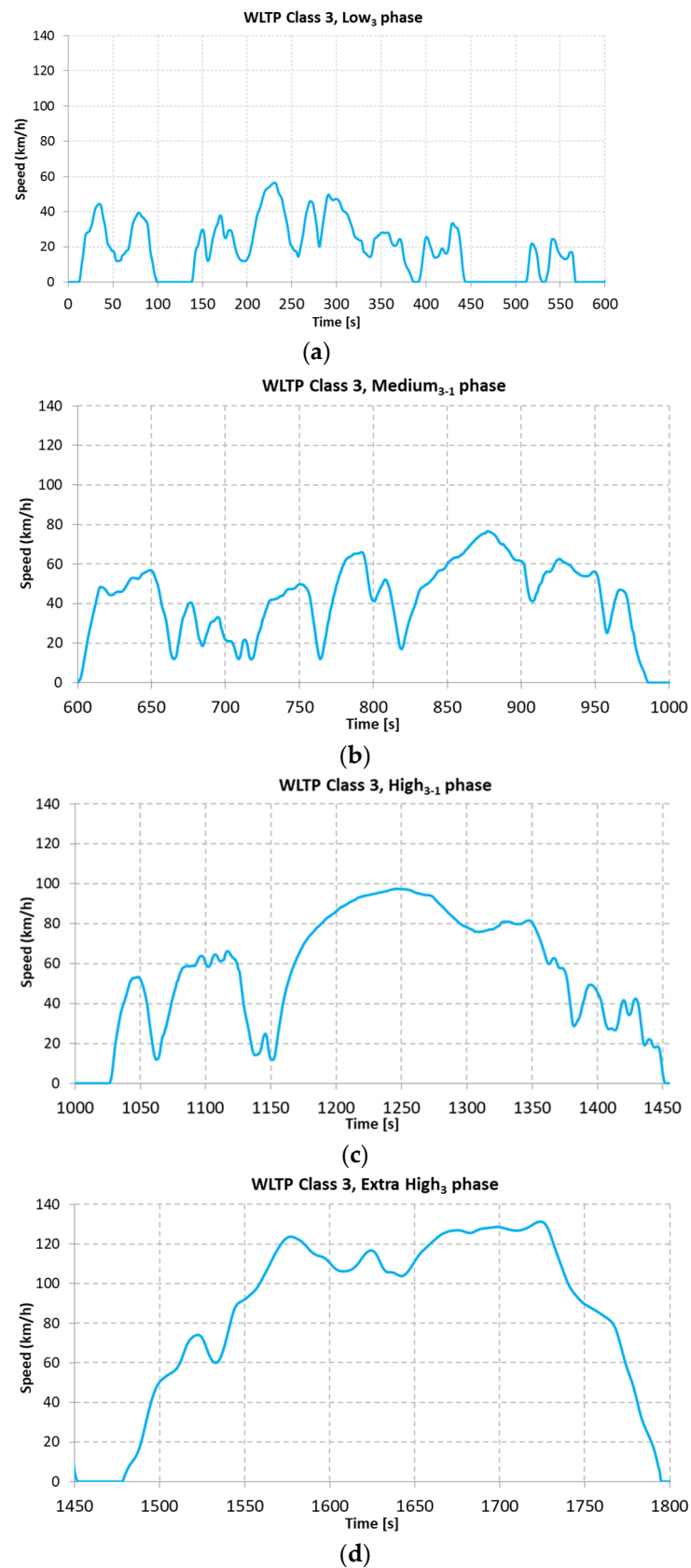


Figure 7. WLTP test cycle, in accordance with Commission Regulation (EU) 2017/1151 [33], where: (a) phase Low₃(A1/7); (b) Medium₃₋₁(A1/8) phase; (c) phase High₃₋₁(A1/10); and (d) Extra High₃ phase (A1/12).

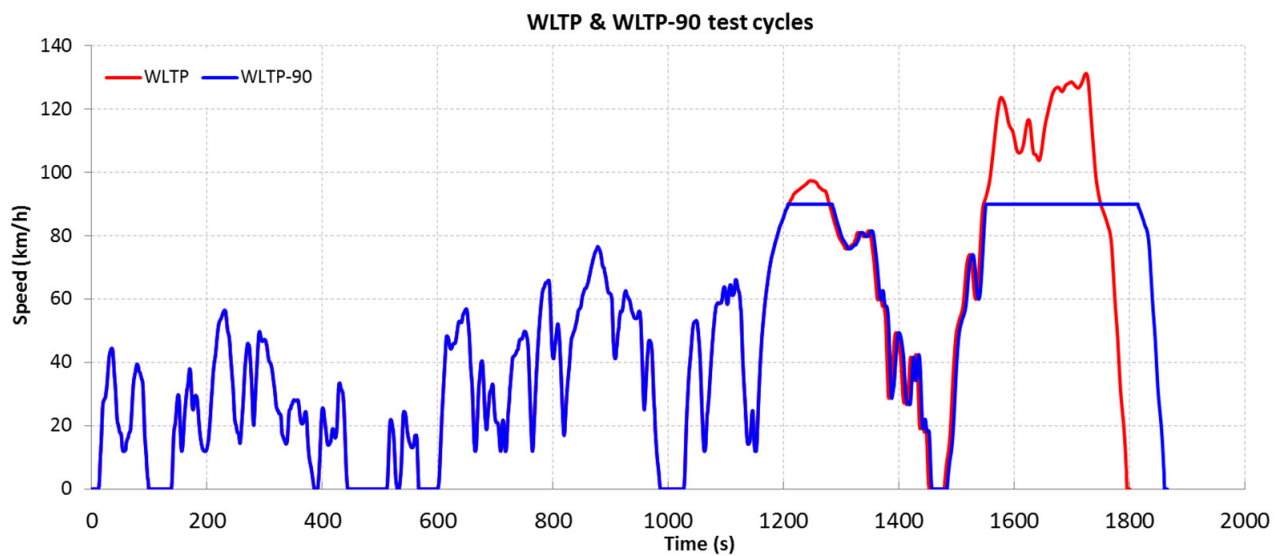


Figure 8. WLTP and WLTP-90 tests profiles.

A different test cycle in relation to WLTP cycles, where only the speed is set for the vehicle at a certain time, is the City Flat Road test. In the test developed by the authors, not only the speed in a given time is set, but also the slope of the terrain and the height of the test route above sea level (Figure 9). The City Flat Road test procedure is therefore close to real road conditions.

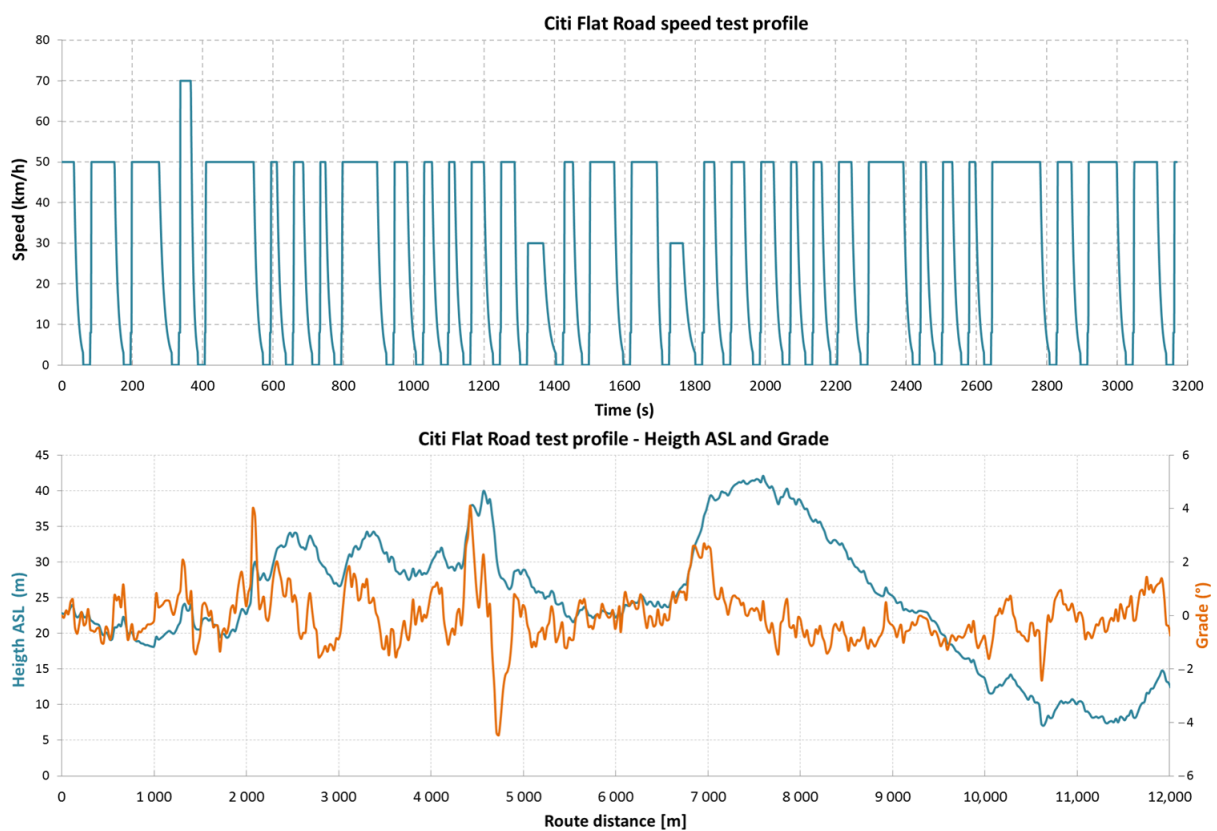


Figure 9. City Flat Road test profile (speed, absolute altitude, and grade).

3. Modeling

Simulations on the model were carried out in the MODELICA environment [34]. The Modelica language enables the modeling of cyber-physical systems, thanks to the ability to

combine components described by mathematical equations and physical relationships to facilitate modeling. The object orientation of the structure enables the use of component models in libraries to use for modeling complex systems containing, for example, mechanical, electrical, electronic, magnetic, hydraulic, and thermal components as well as control principles and methods [34].

Figure 10 shows a model of a delivery vehicle with an electric 4×4 drive system.

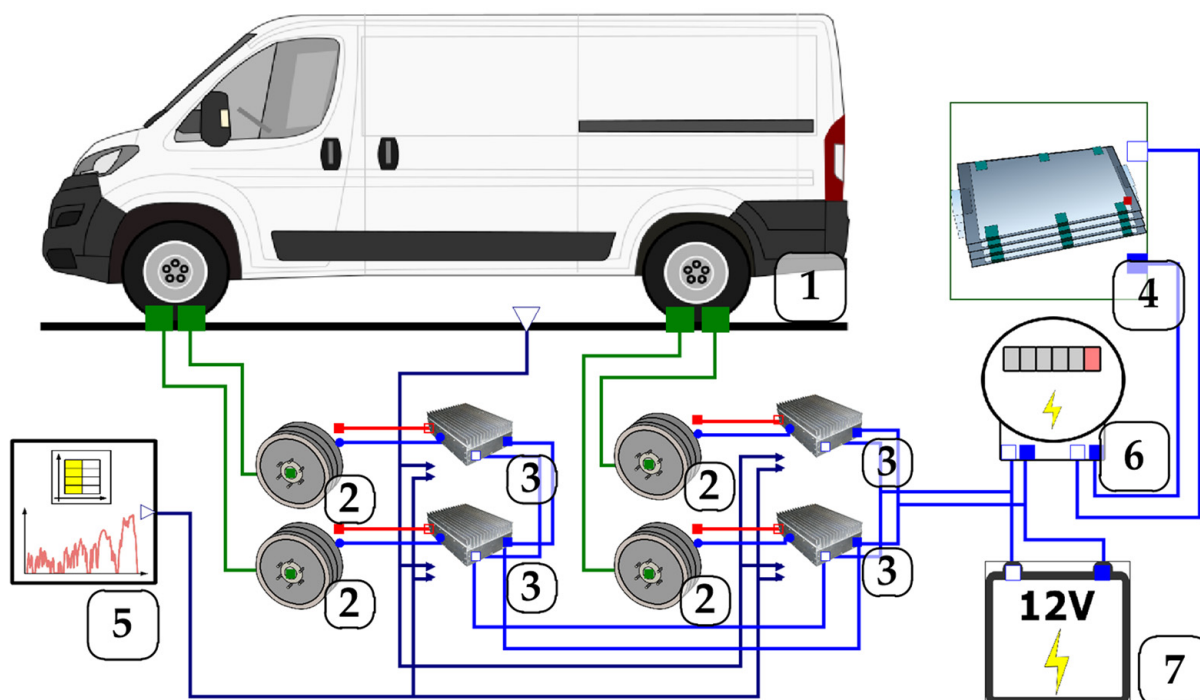


Figure 10. View of the simulation model of a vehicle with an electric 4×4 drive system, divided into blocks: 1—vehicle motion resistance; 2—synchronous motors; 3—voltage inverters; 4—energy storage; 5—travel route adjuster; 6—vehicle cabin heating/cooling system; 7—electric load on the vehicle's on-board system receivers 12VDC.

The developed mathematical model of a vehicle with an electric drive reflects the work of subsystems and modules included in the considered vehicle as a whole, such as:

- the vehicle body with the forces acting on it,
- electric drive system consisting of a synchronous motor module, an inverter module, and an electricity storage module,
- transmission system—automatic gearbox with differential,
- the module for setting the route to be traveled by the vehicle,
- module for setting temperature parameters of the external environment,
- vehicle loading status setting module,
- a module of the thermal conditioning system for the elements of the electric drive system and the passenger compartment together with the ventilation system, consisting mainly of the heat pump module, a bus of valves controlling the flow of heat energy, and heat exchangers,
- module simulating the operation of on-board devices (low-voltage installation of the vehicle, vehicle lighting system, power supply for the terminal of the logistics company system, tachograph power supply, power supply for the audio system, power supply for 12VDC sockets in the vehicle cabin, interior lighting of the vehicle cabin and cargo area, lighting of the vehicle charging sockets, support system steering system, braking system, on-board computer, diagnostic system, monitoring system, etc.),
- measurement module.

The model of the motor built into the wheel hub [35–37], a synchronous machine with permanent magnets, reproduces the behavior of the motor together with the necessary sensors. To develop this model, a model of a synchronous machine with excitation from permanent magnets, derived from the standard library of the Modelica environment, was used.

The inverter model block includes both the converter model, i.e., the voltage inverter, and the FOC control system. This block is one of the most important elements of the modeled electric drive system of the vehicle. The adopted method of control has a fundamental impact on the parameters obtained by the vehicle's electric drive system. The developed voltage inverter block consists of the following elements: a vehicle linear speed controller, a motor current controller, a power electronic converter controller, a current set point value rise limiter unit, an excitation control source selection block, and a block determining the overall efficiency of the motor-inverter system.

The energy storage model with a thermal conditioning system was implemented on the basis of the Modelica Energy Storages library. The developed energy storage model simulates such values as the variable electromotive force of cells; the amount of electrical charge in the cells and the associated state of charge (SOC); variable internal resistance, depending on the temperature of the cells and their state of charge; the temperature of the cells, which is affected by energy lost on the internal resistance, heat flow from the energy storage to the environment, and the heat stream (cooling or heating) coming from the thermal conditioning system of the energy storage, as well as ambient temperature and its interaction with the energy storage. For the energy storage model, the possibility of cooperation with the thermal conditioning system, i.e., supplying or receiving the appropriate amount of heat, was modeled. The supply of heat to the energy storage is modeled for a situation when the ambient temperature drops below a predetermined value and the vehicle itself is connected to the power grid. In this situation, the energy storage is heated by a thermal conditioning system. It is also possible to model heat removal from the energy storage when its temperature rises above 50 °C. Such a phenomenon may occur when the ambient temperature exceeds 35 °C and the drive system itself is operated very intensively. The energy storage model also has the ability to simulate heat exchange with the environment depending on the speed of the vehicle.

The EMF of the energy storage depends on the state of charge of individual cells and was modeled on the basis of the characteristics identified during tests for LFP and NMC cells.

The route-setting block is responsible for controlling the speed of the vehicle while traversing the route, and for providing data on the temporary inclination of the road on which the vehicle is moving. The source of data about speed and inclination are defined in files containing, in the case of inclination, data about the absolute height in m.a.s.l. and inclination in degrees at given waypoints defined by the distance from the starting point. Intermediate values between the points of the given route are subject to linear interpolation in such a way that the functions of absolute height and road slope are continuous. Thanks to this, the information about the traveled distance can be taken from the block of resistances to vehicle motion. The speed at which the vehicle is to move on a given road section is also defined in the form of a text file. The file describing the speed of the vehicle as a function of time contains pairs of points in the format (time (s), speed (km/h)) in one-second intervals. This is a common format for the description of synthetic road tests used to assess the energy consumption of vehicles, used e.g., by the United States Environmental Protection Agency [38].

Taking into account the estimation errors, the total weight of the vehicle was assumed for the simulation tests, depending on the type of cell chemistry used. The parameters adopted in the simulation are presented in Table 3.

Table 3. Vehicle parameters.

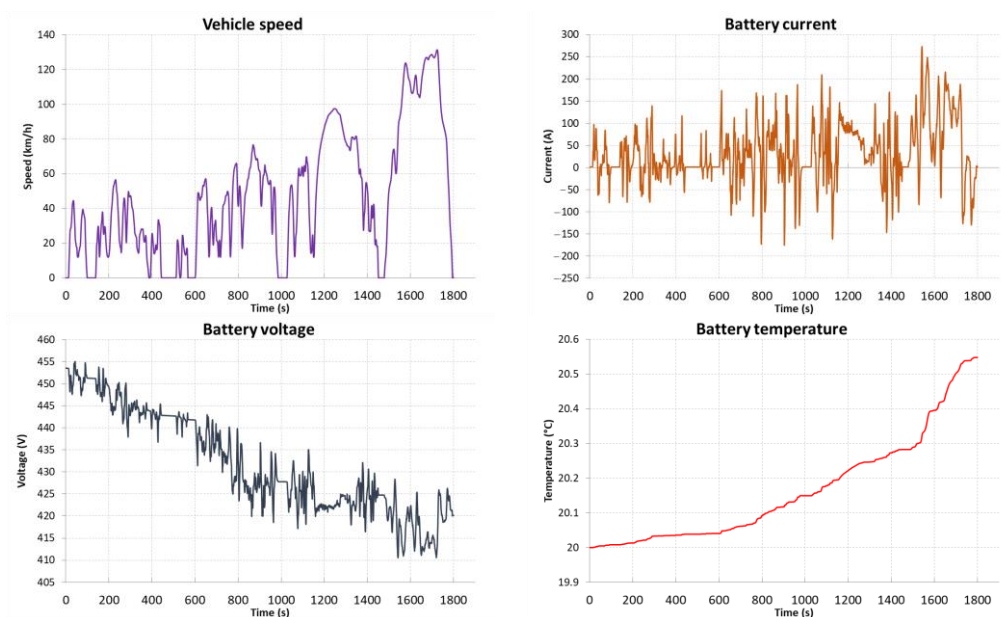
| Parameter | Value |
|--|------------------------|
| Vehicle Mass, ES Type 1 (kg) | 3974 |
| Vehicle Mass, ES Type 2 (kg) | 3498 |
| Vehicle Mass, ES Type 3 (kg) | 3478 |
| Usable Energy, all ES types (kWh) | 60 |
| Nominal motor power (kW) | 4 × 60 |
| Nominal motor torque (Nm) | 800 |
| Nominal motor RPM | 715 |
| Vehicle frontal area (m ²) | 3.99 |
| Drag coefficient (–) | 0.31 |
| Tyre size | 195/75 R16 110/108 R C |

4. Results

4.1. Research on Energy Consumption Using LFP Cells—Type 1

The tests were carried out using the mathematical model of the drive system described in Section 2. A Type 1 energy storage was used, based on 126 LFP prismatic cells with a capacity of 160 Ah. The available usable energy contained in this storage is 60 kWh, with a reserve of 7.0% (4.61 kWh). The presence of the reserve protects the energy storage cells against complete discharge, which also contributes to extending their service life. The tests were carried out for two ambient temperatures of 0 °C and 20 °C, however, due to the volume of the obtained results, the test results for the temperature of 20 °C are presented, while the key values for both temperatures, such as energy consumption and range, are presented in the form of tables.

Figure 11 shows the results of the simulation of the full WLTP test cycle, lasting 1800 s. Figure 12 shows the results for the modified WLTP-90 test cycle, during which the vehicle speed is limited to 90 km/h and the test duration is 1861 s. Figure 13 test results for the actual City Flat Road test route, 24.3 km long, are presented. The test was conducted at a simulated ambient temperature of 20 °C.

**Figure 11.** Cont.

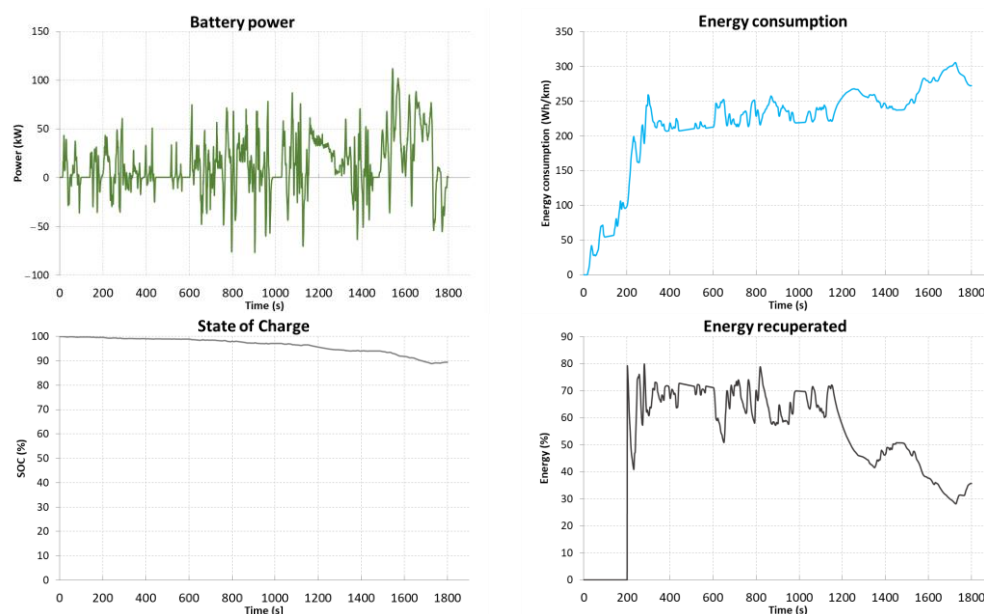


Figure 11. WLTP results of simulation tests for the 4 × 4 drive system with Type 1 energy storage.

In Figure 11 the results of the WLTP test of a 4 × 4 equipped with Type 1 energy storage (LFP prismatic cells) are shown. The range on a fully charged energy storage is 229.3 km, with an average energy consumption of 272.2 W/km. The profile of this test is relatively strenuous due to the driving speed required, which translates into energy consumption. The test results indicate a high current load on the storage, especially in the final phase of the test cycle when the instantaneous values reach 250 A, which is related to the high speed of the vehicle. One characteristic of this test is also a rapid increase in battery temperature in a short time, for the Type 1 energy storage it was 0.55 °C, and in the final phase of the test, the increase was over 0.3 °C in the last 300 s.

The WLTP-90 test (Figure 12) is a milder version of the WLTP test with a speed limit of 90 km/h. This has a significant impact on power consumption and range. In the WLTP-90 test with Type 1 energy storage, the range of the vehicle is 251.6 km, and the energy consumption is 249.9 W/km. The warehouse load is also lower than in the previous one, which results in a milder temperature increase during the test cycle, amounting to 0.36 °C, and much milder in the last phase of 0.11 °C in 300 s.

In the Test City Flat Road test (Figure 13), a range of 279.4 km was achieved with an energy consumption of 223.6 W/km. The energy storage during tests in this profile of use is evenly loaded with the current due to the relatively low speed, frequent braking, and acceleration, which allows for a relatively high energy recovery of 56.3%. The operating temperature of the batteries increased by 0.9 °C over the entire test cycle in a linear manner.

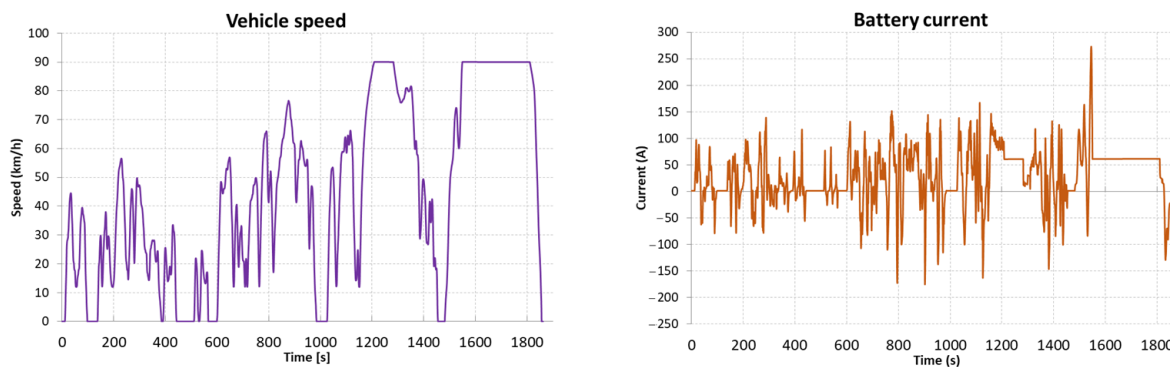


Figure 12. Cont.

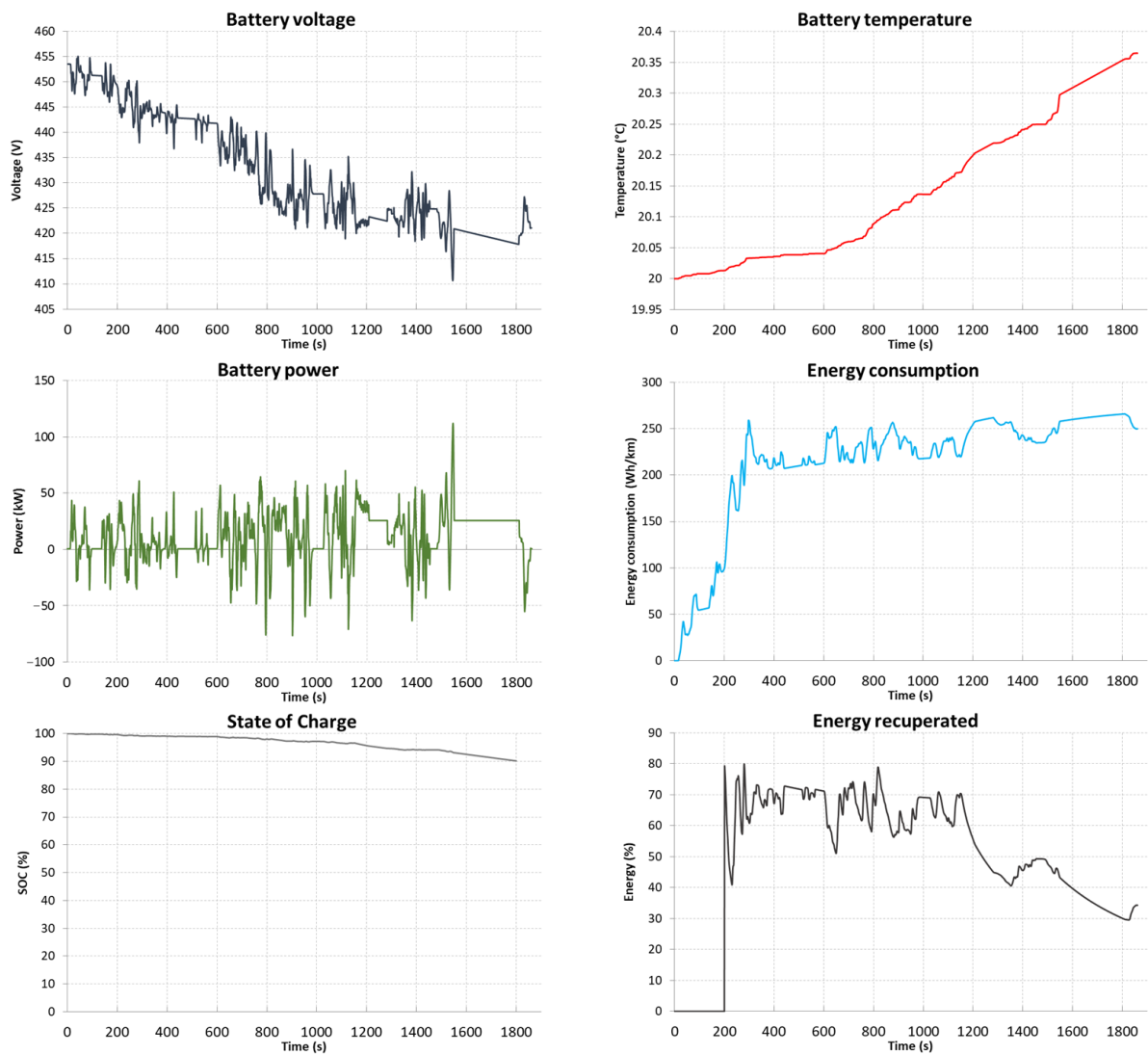


Figure 12. WLTP-90 results of simulation tests for the 4 × 4 drive system with Type 1 energy storage.

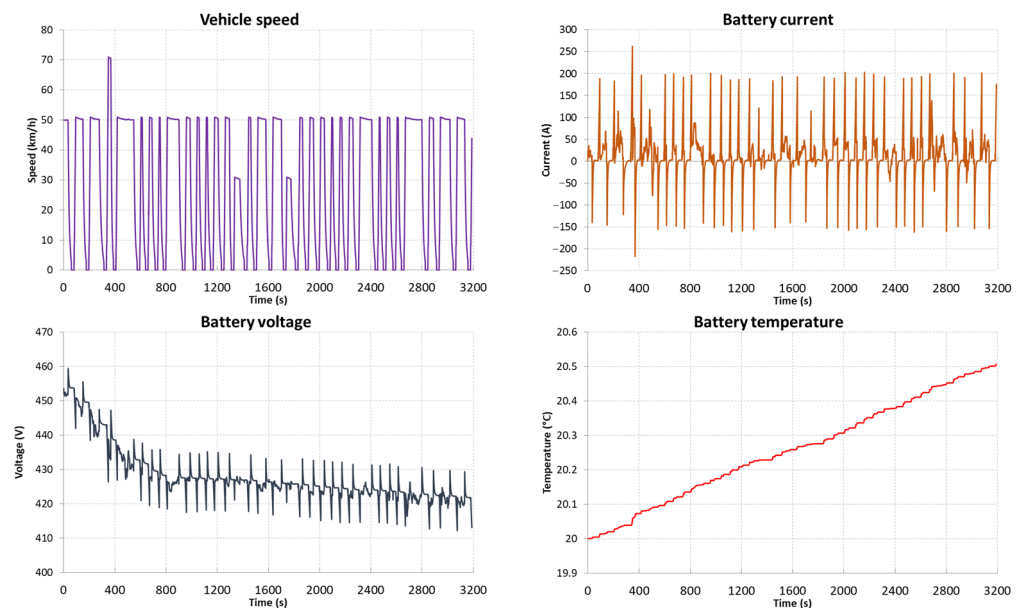


Figure 13. Cont.

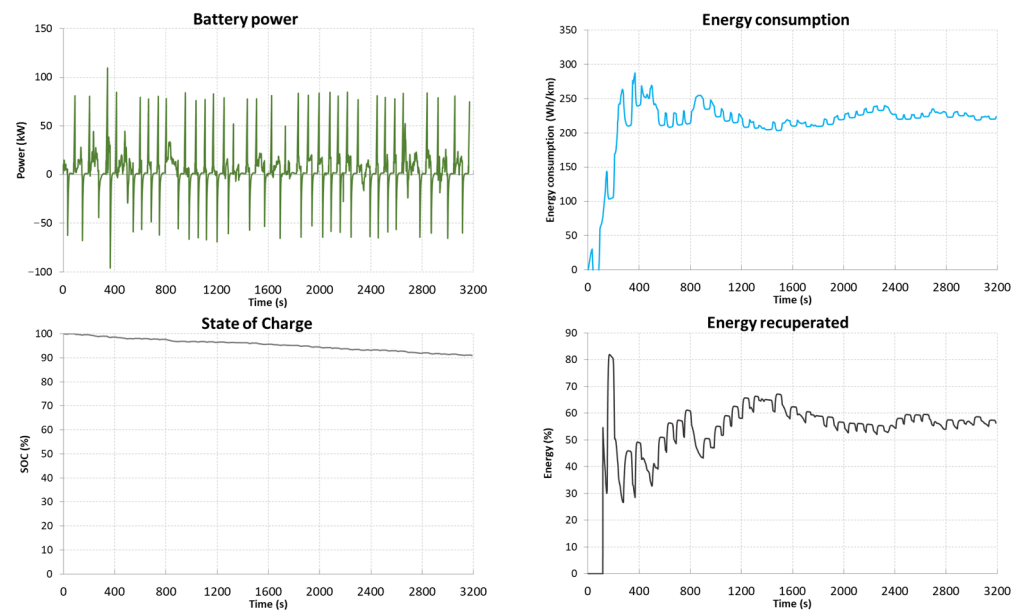


Figure 13. City Flat Road results of simulation tests for the 4×4 drive system with Type 1 energy storage.

4.2. Research on Energy Consumption Using NMC Cylindrical Cells—Type 2

The tests were carried out using the mathematical model of the drive system described in Section 2. A Type 2 energy storage was used, based on 6048 pieces of NMC cells in size 18,650. 54 cells with a capacity of 3.0 Ah were connected in parallel into modules, which were then connected in a series in the number 112. The available usable energy contained in this store was 60 kWh, with an unused reserve of 8.1% (5.32 kWh).

Figure 14 shows the results of the simulation of the full WLTP test cycle, lasting 1800 s. Figure 15 shows the results for the modified WLTP-90 test cycle, where the speed is limited to 90 km/h and the test duration is 1861 s. Figure 16 test results for the actual City Flat Road test route, 24.3 km long, are presented. The test was conducted at a simulated ambient temperature of 20 °C.

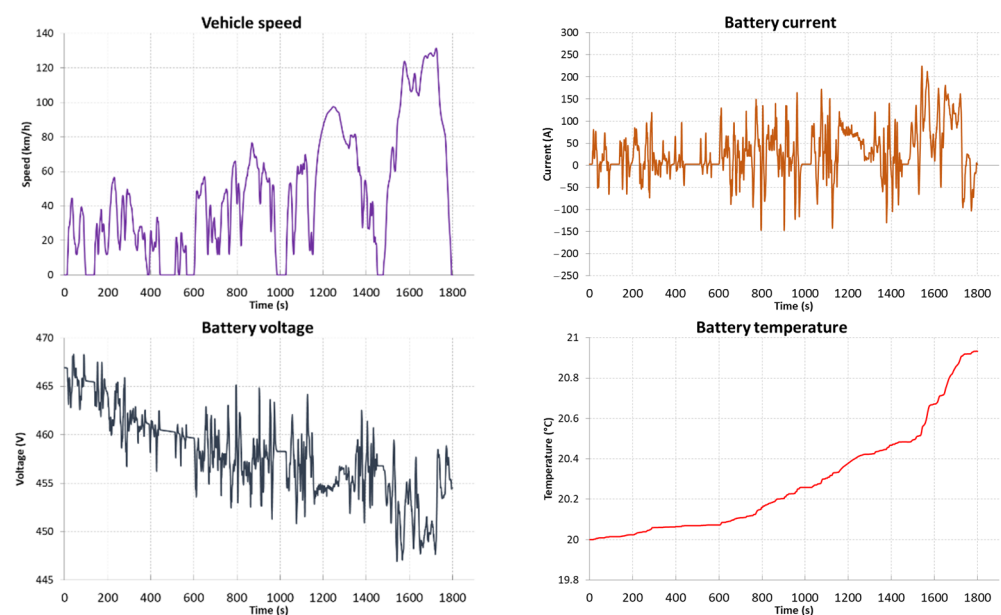


Figure 14. Cont.

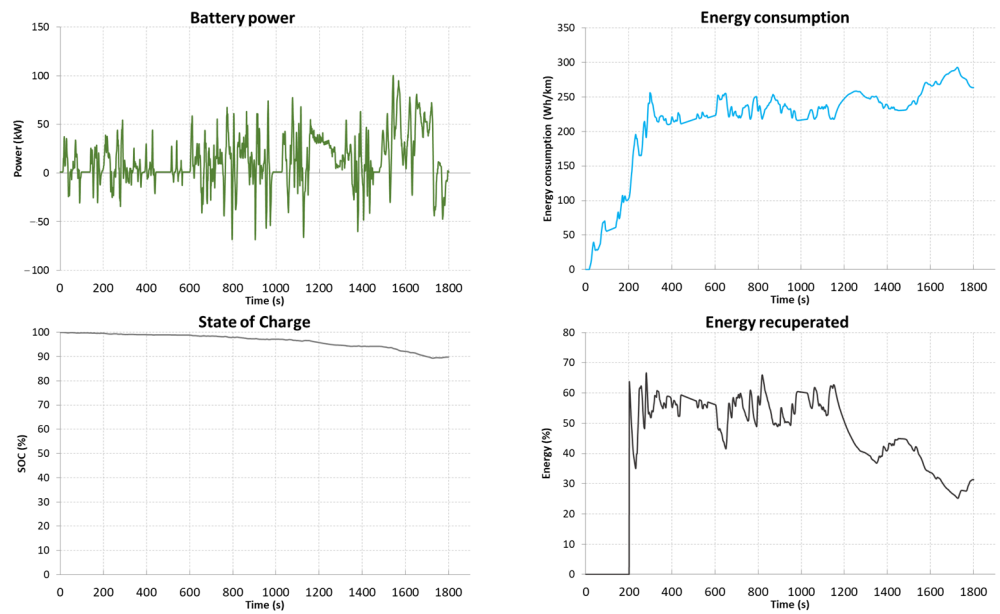


Figure 14. WLTP results of simulation tests for the 4 × 4 drive system with Type 2 energy storage.

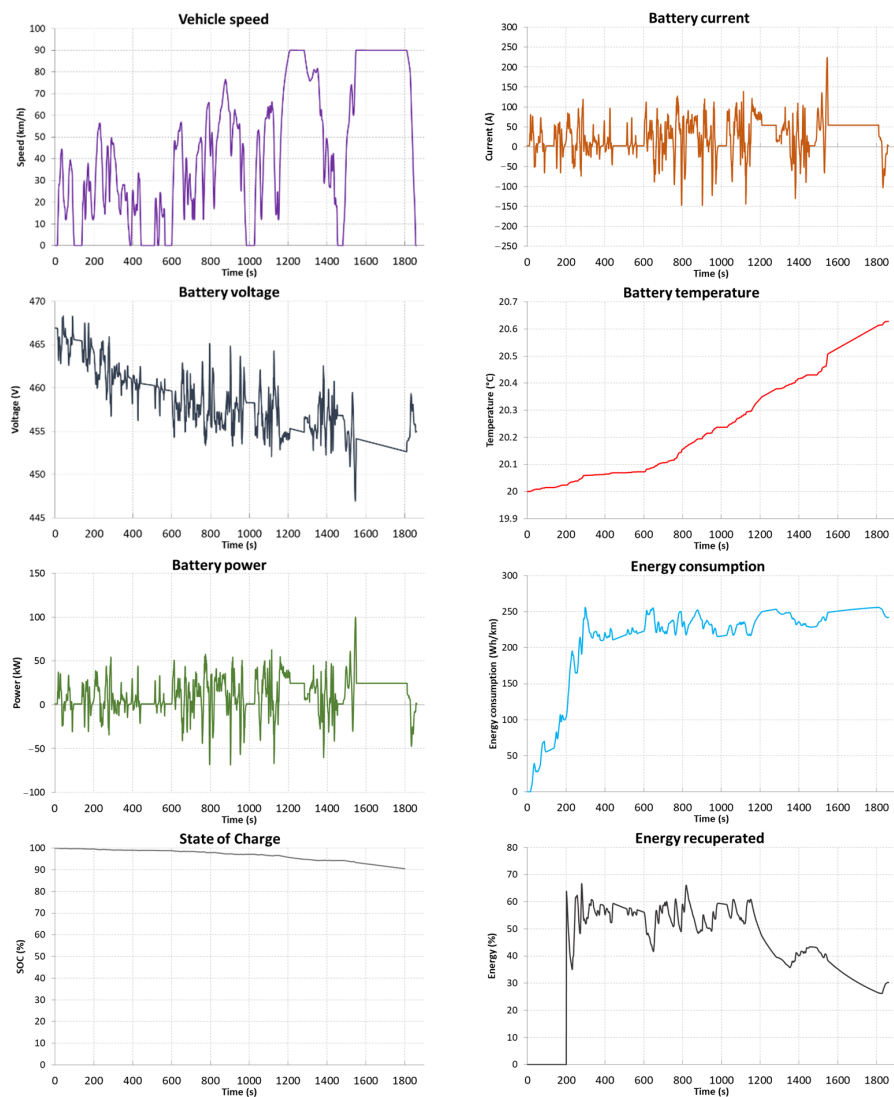


Figure 15. WLTP-90 results of simulation tests for the 4 × 4 drive system with Type 2 energy storage.

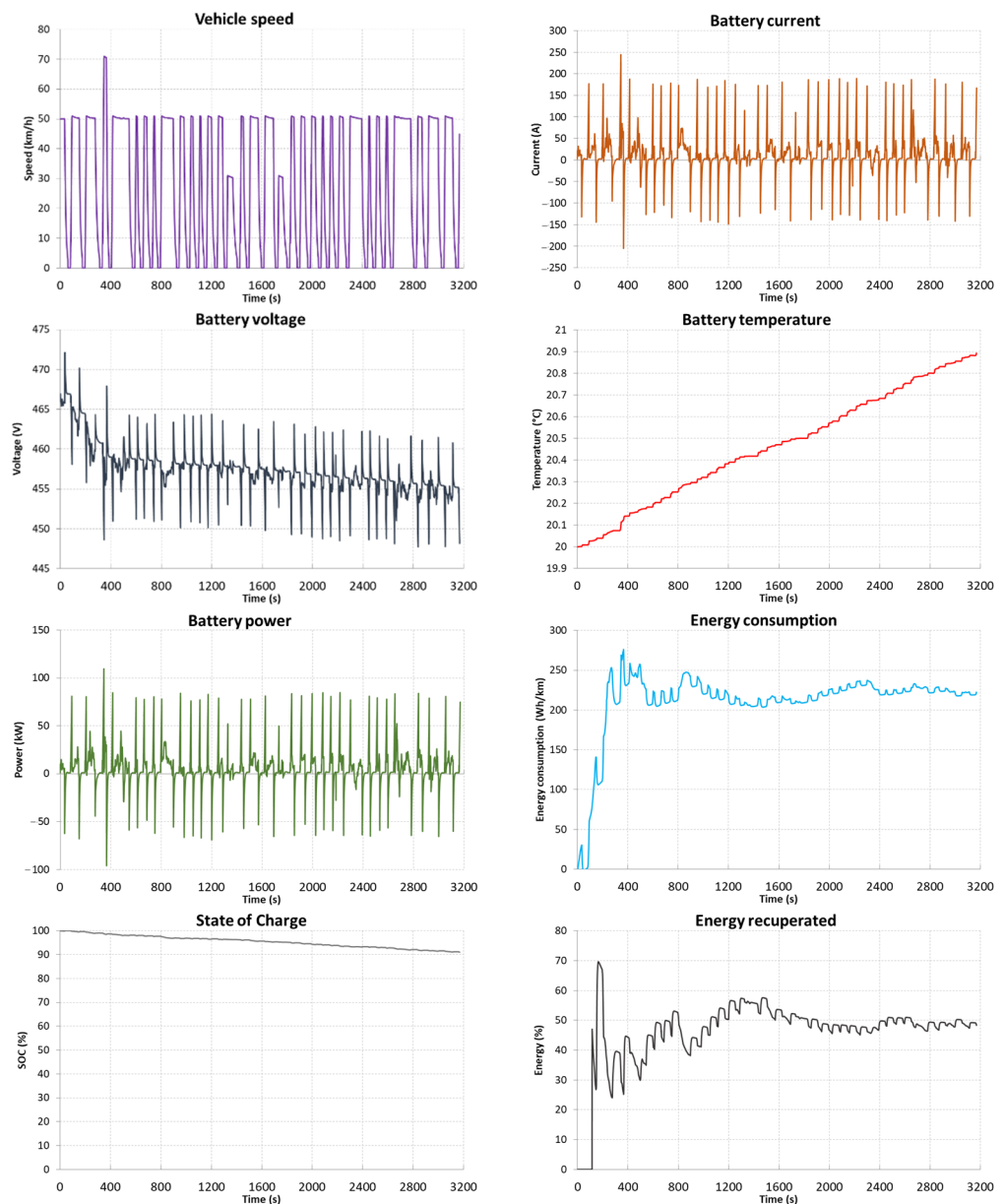


Figure 16. City Flat Road results of simulation tests for the 4×4 drive system with Type 2 energy storage.

Figure 14 presents the results of the WLTP test of a 4×4 vehicle equipped with Type 2 energy storage (cylindrical NMC cells). The range of full energy storage is 255.3 km, with an average energy consumption of 263.4 W/km. The test profile is characterized by a high current load of the storage, whose instantaneous values exceed 220 A. A characteristic feature of this test is a rapid increase in battery temperature, in the case of cylindrical cells used to build this type of storage, it is over $1.9 \text{ }^\circ\text{C}$ throughout the WLTP cycle, and in the last phase of the cycle of more than $0.8 \text{ }^\circ\text{C}$ in 300 s).

In the WLTP-90 test and the Type 2 energy storage (Figure 15), the range of the vehicle is 278.9 km with an average energy consumption of 241.9 Wh/km. Energy consumption in this driving profile is 5.62 kWh and recovery is 1.70 kWh (30%). The temperature of the batteries during the test cycle increased by $1.62 \text{ }^\circ\text{C}$, $0.35 \text{ }^\circ\text{C}$ in the last phase of the test.

The test in the City Flat Road cycle (Figure 16) with the tested Type 2 energy storage allowed to drive 302.1 km with a consumption of 222.5 Wh/km. In the observed driving profile, an increase in temperature during the test cycle of $0.9 \text{ }^\circ\text{C}$ was observed in a linear

manner. Similar to the previous type of energy storage, this test profile allowed for the highest energy recovery in the Type 2 storage and it is at the level of 39%.

4.3. Research on Energy Consumption Using NMC Cells (Pouch)—Type 3

The tests were carried out using the mathematical model of the drive system described in Section 2. A Type 3 energy storage was used, based on 236 NMC pouch cells. The storage is made of modules of 2 cells connected in parallel, and then of 118 modules connected in a series. The available usable energy contained in this storage was 60 kWh, with an unused reserve of 7.1% (4.57 kWh).

Figure 17 shows the results of the simulation of the full WLTP test cycle, lasting 1800 s. Figure 18 shows the results for the modified WLTP-90 test cycle, for a vehicle with a design speed limited to 90 km/h, with a duration of 1861 s. In turn, Figure 19 shows the test results for the actual City Flat Road test route, 24.3 km long. The test was conducted at a simulated ambient temperature of 20 °C.

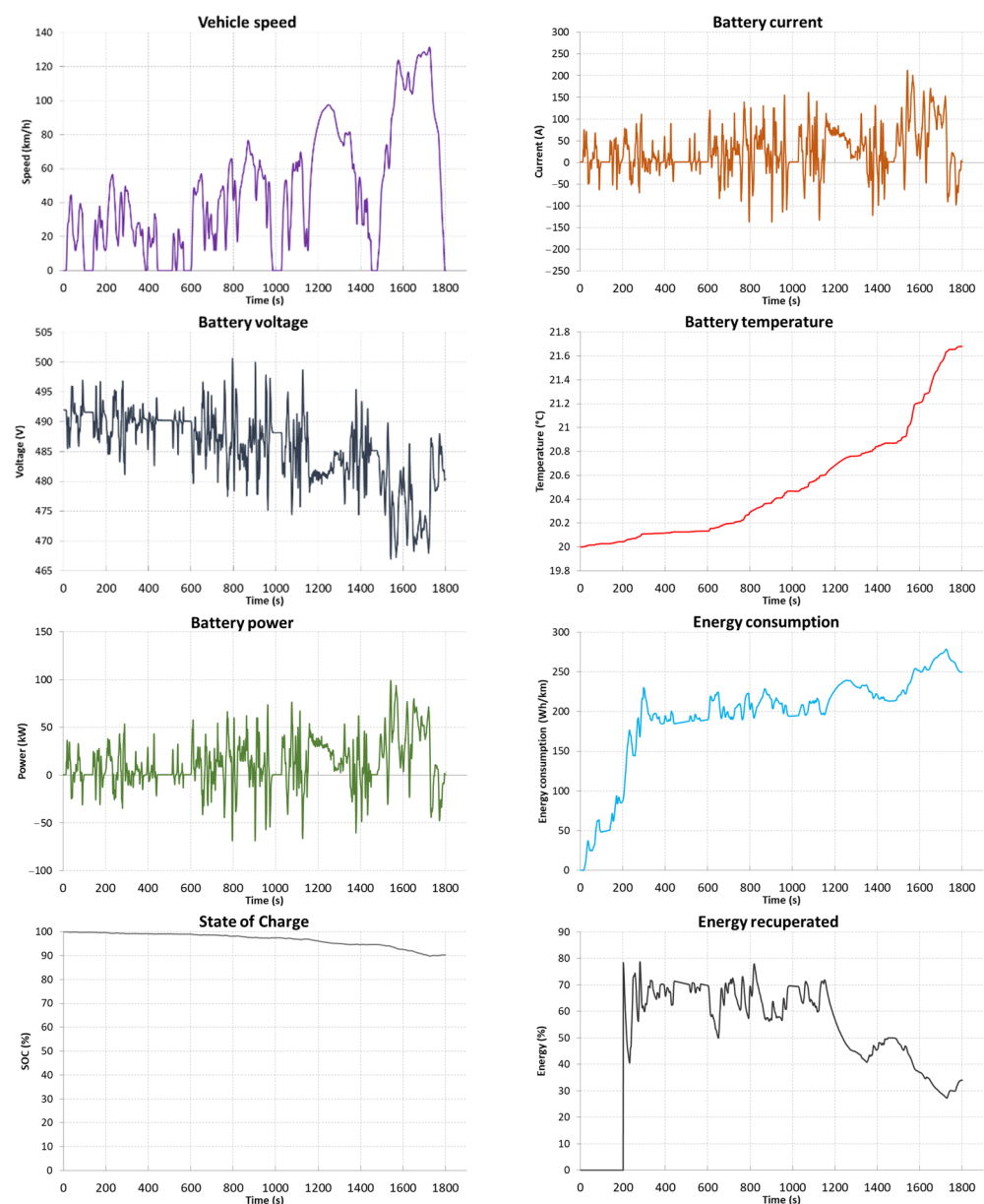


Figure 17. WLTP results of simulation tests for the 4 × 4 drive system with Type 3 energy storage.

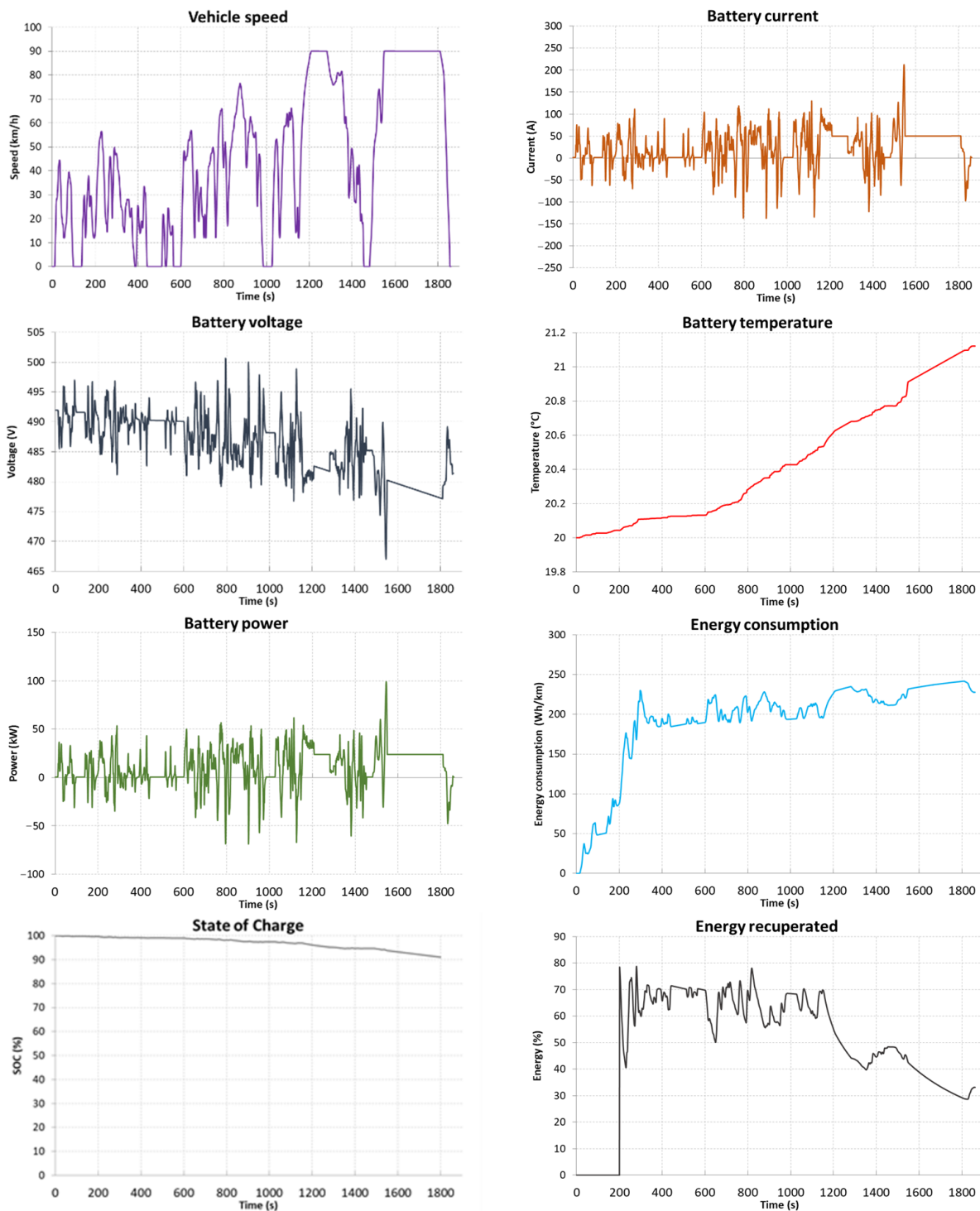


Figure 18. WLTP-90 results of simulation tests for the 4×4 drive system with Type 3 energy storage.

The graphs above (Figure 17) show the dependencies regarding the test of a 4×4 vehicle with a Type 3 warehouse in the WLTP tests. The range of the vehicle in this test is 268.7 km and the average energy consumption is 249.7 Wh/km. The energy used in the cycle is 5.81 kWh and the energy recovered is 1.98 kWh (34%). The temperature increase during the test cycle is 1.7 °C, but in the last phase of the test, it is an increase of 1 °C in 300 s.

In the WLTP-90 test (Figure 18) with the Type 3 energy storage, the range was 296.6 km with an average energy consumption of 227.7 Wh/km. With the energy used in the cycle of

5.62 kWh, the energy recovered is 1.70 kWh (30.2%). The temperature increase in the test cycle is 1.1 °C, in the last 300 s the increase was 0.3 °C.

In the City Flat Road test (Figure 19), the range was 335.4 km with an average energy consumption of 100.6 Wh/km. The energy used in the cycle is 4.84 kWh and the energy recovered is 2.71 kWh (56%). The temperature increase during the test cycle is 1.6 °C and is characterized by a linear increase in time.

Table 4 contains data on energy consumption in Wh/km and range in km, obtained as a result of simulations for three test routes, for the ambient temperature and the initial temperature of the energy storage equal to 20 °C (Figures 10–18). Table 5 shows analogous data for ambient temperatures and initial energy storage of 0 °C.

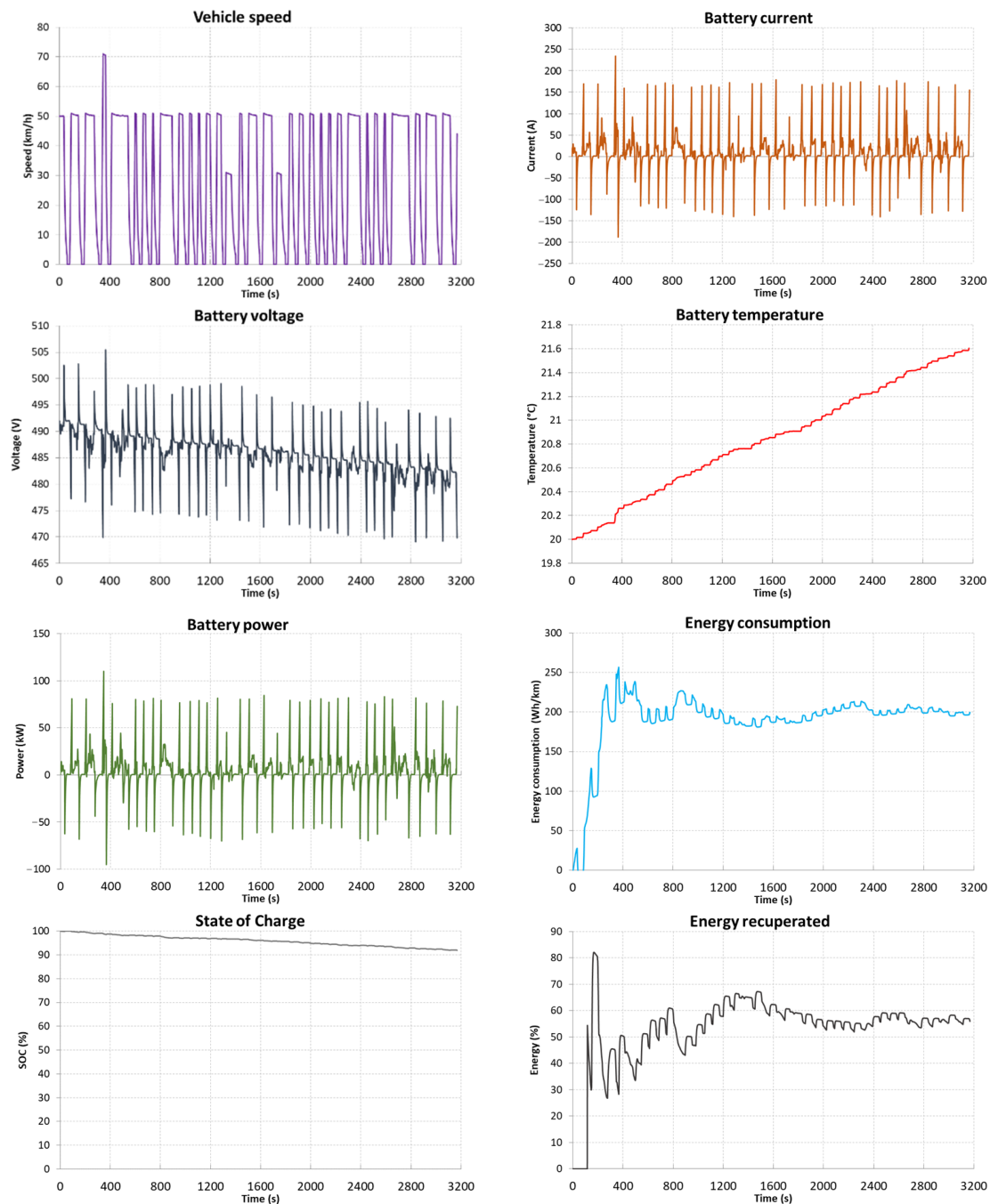


Figure 19. City Flat Road results of simulation tests for the 4 × 4 drive system with Type 3 energy storage.

Table 4. Vehicle energy consumption and range, at 20 °C ambient temperature.

| ES Type and Test Cycle | Energy Consumption (Wh/km) | Vehicle Range (km) |
|---------------------------|----------------------------|--------------------|
| WLTP, ES Type 1 | 272.29 | 229.25 |
| WLTP, ES Type 2 | 263.39 | 255.26 |
| WLTP, ES Type 3 | 249.65 | 268.68 |
| WLTP-90, ES Type 1 | 249.89 | 251.56 |
| WLTP-90, ES Type 2 | 241.95 | 278.98 |
| WLTP-90, ES Type 3 | 227.74 | 296.59 |
| City Flat Road, ES Type 1 | 223.59 | 279.45 |
| City Flat Road, ES Type 2 | 222.46 | 302.05 |
| City Flat Road, ES Type 3 | 199.61 | 335.36 |

Table 5. Vehicle energy consumption and range, at 0 °C ambient temperature.

| ES Type and Test Cycle | Energy Consumption (Wh/km) | Vehicle Range (km) |
|---------------------------|----------------------------|--------------------|
| WLTP, ES Type 1 | 293.74 | 204.56 |
| WLTP, ES Type 2 | 284.88 | 233.86 |
| WLTP, ES Type 3 | 271.14 | 239.43 |
| WLTP-90, ES Type 1 | 272.16 | 224.43 |
| WLTP-90, ES Type 2 | 264.23 | 253.70 |
| WLTP-90, ES Type 3 | 250.02 | 263.55 |
| City Flat Road, ES Type 1 | 260.06 | 231.32 |
| City Flat Road, ES Type 2 | 258.74 | 257.43 |
| City Flat Road, ES Type 3 | 235.87 | 274.48 |

Table 6 shows data related to the amount of energy used during the test cycle and the energy recovered by regenerative braking, for test cycles conducted at a temperature of 20 °C. Data at 0 °C are shown in Table 7.

Table 6. Vehicle energy consumed and recuperated, at 20 °C ambient temperature.

| ES Type and Test Cycle | Energy Consumed (kWh) | Energy Recuperated (kWh) | Recuperation Percentage (%) |
|---------------------------|-----------------------|--------------------------|-----------------------------|
| WLTP, ES Type 1 | 6.34 | 2.26 | 35.67 |
| WLTP, ES Type 2 | 6.13 | 1.92 | 31.34 |
| WLTP, ES Type 3 | 5.81 | 1.98 | 34.03 |
| WLTP-90, ES Type 1 | 5.80 | 1.99 | 34.31 |
| WLTP-90, ES Type 2 | 5.62 | 1.70 | 30.27 |
| WLTP-90, ES Type 3 | 5.29 | 1.75 | 33.16 |
| City Flat Road, ES Type 1 | 5.42 | 3.05 | 56.32 |
| City Flat Road, ES Type 2 | 5.39 | 2.61 | 48.32 |
| City Flat Road, ES Type 3 | 4.84 | 2.71 | 55.96 |

Table 8 presents a summary of the potentially achievable range of a vehicle with a given type of battery in a situation where they were operated to a certain level of charge DOC and discharge DOD.

Table 7. Vehicle energy consumed and recuperated, at 0 °C ambient temperature.

| ES Type and Test Cycle | Energy Consumed (kWh) | Energy Recuperated (kWh) | Recuperation Percentage (%) |
|---------------------------|-----------------------|--------------------------|-----------------------------|
| WLTP, ES Type 1 | 6.83 | 2.15 | 31.39 |
| WLTP, ES Type 2 | 6.63 | 1.81 | 27.35 |
| WLTP, ES Type 3 | 6.31 | 1.86 | 29.54 |
| WLTP-90, ES Type 1 | 6.32 | 1.88 | 29.82 |
| WLTP-90, ES Type 2 | 6.13 | 1.60 | 26.08 |
| WLTP-90, ES Type 3 | 5.80 | 1.65 | 28.40 |
| City Flat Road, ES Type 1 | 6.31 | 2.86 | 45.36 |
| City Flat Road, ES Type 2 | 6.27 | 2.44 | 38.90 |
| City Flat Road, ES Type 3 | 5.72 | 2.52 | 44.10 |

Table 8. Total achievable range for different types of energy storage -WLTC test at 20 °C ambient temperature.

| Charge/Discharge Level | ES Type 1 (km) | ES Type 2 (km) | ES Type 3 (km) |
|------------------------|----------------|----------------|----------------|
| 0–100% | 440,705 | 56,038 | 90,366 |
| 10–90% | 881,409 | 74,718 | 127,276 |
| 20–80% | 1,057,691 | 203,242 | 306,730 |
| 30–70% | 1,322,114 | 273,359 | 321,714 |

The method of aggregation of optimization criteria was used to select a given type of cells. Assuming that not all the component criteria $f(x)$ are approximately equally important, the multi-criteria task was replaced with a single-criteria task in the form of:

$$\max_{x \in \Omega} f(x) = \sum_{n=1}^j w_n f_n(x) \quad (12)$$

$$w_n \geq 0; \quad n = 1, 2, \dots, j; \quad w_n \in \langle 0, 1 \rangle; \quad f_n(x) = \frac{f_n}{f_{nmax}}$$

where: x —parametric variables describing a given energy storage parameter; Ω —the area of possible solutions in the space of objects; $f(x)$ —objective function; $f_n(x)$ —a normalized function representing a given criterion; w_n —weighting factor; f_n —the value of the evaluated parameter; f_{nmax} —the maximum value of the evaluated parameter.

On the basis of the above relationship, individual parameters were estimated and evaluated, which made it possible to determine the ranking evaluation of the analyzed types of cells. For the assessment of individual parameters, the best results of a given parameter that can be found in the literature and market offers of manufacturers were adopted [39–42]. Individual weighting factors were selected on the basis of the authors' operational experience. The results of the analyzes carried out are presented in Table 9 and Figure 20 (the calculated values for the normalized function representing the given evaluation criterion, and the final value of the ranked rating for the considered types of energy storages are presented).

The following values were adopted for the individual parameters included in the criteria for assessing the types of energy storage, the results of which are presented in Table 9:

1. Cost: the total cost of the energy storage, estimation assuming an optimal price of 10,000.00 USD
2. Max no. of cycles: the life of the energy storage—assessment assuming the optimal number of cycles at the level of 20,000
3. Energy density: energy density—assessment assuming the maximum energy density of cells available on the market at 360 Wh/kg
4. Reliability: reliability—rating assuming reliability at level 1

5. Mass: total weight of the energy storage—evaluation assuming an optimal storage mass of 200 kg
6. Temperature dependency: the relationship determining the ratio of the internal resistance of the cells for two temperature values 0 °C and 20 °C—the reference value is 1
7. ES temperature conditioning requirements: the requirement to use a thermal conditioning system for a given type of cells—the reference value for a system that does not require a thermal conditioning system is 1
8. Total range: vehicle range obtained from a given type of energy storage during its complete operation from new to disassembly—assessment assuming a total vehicle range of 1,500,000 km.

Based on the analyzes carried out using the optimization criteria aggregation method, the results of which are presented in Table 9 and Figure 20, it was shown that the best energy storage for use in a delivery vehicle is a Type 1 storage using LFP cells.

Table 9. Energy storage types summary.

| Energy Storage | ES Type 1 | ES Type 2 | ES Type 3 |
|---|-------------------------------|---------------------------------------|-------------------------------|
| Cost (USD) $f_{1max} = 10,000$ $w_1 = 0.13; f_1(x) \rightarrow$ | 26,838.00 USD 0.37 0.05 | 49,957.00 USD 0.20 0.03 | 12,500.00 USD 0.80 0.10 |
| Max no. of cycles (80 SOH) $f_{2max} = 20,000$ $w_2 = 0.13; f_2(x) \rightarrow$ | 8000 0.40 0.05 | 3000 0.15 0.02 | 3650 0.18 0.02 |
| Energy density (Wh/kg) $f_{3max} = 360$ $w_3 = 0.13; f_3(x) \rightarrow$ | 81.76 0.23 0.03 | 208.02 0.58 0.08 | 220.38 0.61 0.08 |
| Reliability $f_{4max} = 1$ $w_4 = 0.12; f_4(x) \rightarrow$ | 0.53259 0.53259 0.06 | 0.0000001 0.0000001 0.000000012 | 0.30728 0.30728 0.04 |
| Mass (kg) $F_{5max} = 200$ $w_5 = 0.12; f_5(x) \rightarrow$ | 789 0.25 0.03 | 314 0.64 0.08 | 293 0.68 0.08 |
| Temperature dependency (IR delta 0 °C and 20 °C) $f_{6max} = 0.1$ $w_6 = 0.12; f_6(x) \rightarrow$ | 0.51 0.20 0.02 | 0.57 0.18 0.02 | 0.39 0.26 0.03 |
| ES temperature conditioning requirement $f_{7max} = 1$ $w_7 = 0.12; f_7(x) \rightarrow$ | 1.00 1.00 0.12 | 0.20 0.20 0.02 | 0.40 0.40 0.05 |
| Total range (km) $f_{8max} = 1,500,000$ $w_8 = 0.13; f_8(x) \rightarrow$ | 1,322,114 0.88 0.11 | 273,359 0.18 0.02 | 321,714 0.21 0.03 |
| Ranked rating $f_n(x) = \sum\{f_1(x) \div f_8(x)\}$ | 0.48 | 0.27 | 0.43 |

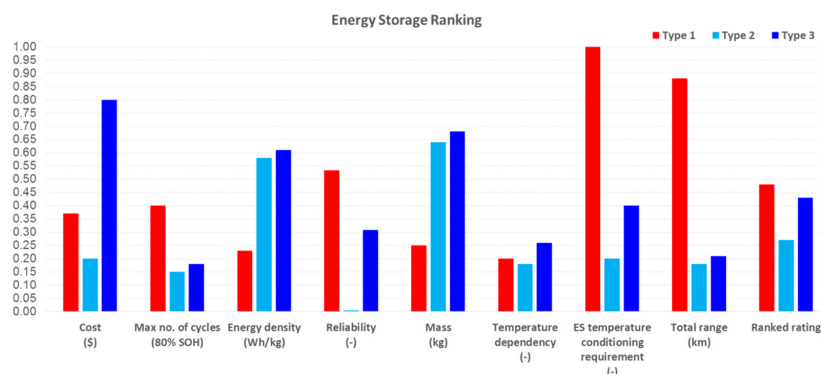


Figure 20. Ranking of energy storage types.

5. Discussion

The analysis of the parameters obtained by a 4×4 vehicle using three different energy storage systems operating at an ambient temperature of $20\text{ }^{\circ}\text{C}$ (summer period, moderate climate) and $0\text{ }^{\circ}\text{C}$ (winter period, moderate climate in Europe) shows a decrease in the range of the vehicle in the presence of lower temperatures. This value is associated with a change in the initial temperature of the energy storage and thus an increase in the internal resistance of the cells. For the Type 1 energy storage, the range decreased by 10.77%, for Type 2 by 8.38%, and for Type 3 by 10.89%.

The test results obtained at lowering the ambient temperature for the WLTP-90 test route, where the maximum speed is limited to 90 km/h, are comparable and amount to: Type 1 decreasing by 10.78%, Type 2 decreasing by 9.06%, and Type 3 decreasing by 11.14%.

For the actual City Flat Road, there are larger differences in the drop from $20\text{ }^{\circ}\text{C}$ to $0\text{ }^{\circ}\text{C}$ respectively: Type 1 decreases by 17.22%, Type 2 decreases by 14.77%, and Type 3 decreases by 18.15%.

The decrease in the range when the temperature of the energy storage based on lithium cells decreases is an inevitable phenomenon resulting from the increase in the internal resistance of the storage cells. It can be prevented by using appropriate energy storage thermal conditioning systems that use the possibility of connecting the vehicle to the power grid or to the energy storage itself during the operation of the vehicle. Unfortunately, not all manufacturers of electric vehicles install such systems in order to optimally maintain the temperature of the energy storage. In addition, regardless of the type of energy storage, the operation of the vehicle in the autumn-winter-spring period, when ambient temperatures fall below $15\text{ }^{\circ}\text{C}$, requires heating the passenger compartment, which entails increased energy consumption and a decrease in the vehicle's range. It can be argued that the range of optimal temperatures in which electrochemical energy storage should be operated is close to the temperature at which people feel comfortable ($16\text{--}21\text{ }^{\circ}\text{C}$). In order to prevent low temperatures, both for the energy storage and the passenger compartment, heating systems are used that use electric heaters integrated with the energy storage (e.g., plate heaters), electric heaters connected to the cooling circuit of the liquid energy storage, or a heat pump system that uses ambient energy to increase heating efficiency while reducing its consumption from the power source.

The conducted tests of the vehicle's electric drive system in the presence of two selected temperature levels, i.e., $0\text{ }^{\circ}\text{C}$ and $20\text{ }^{\circ}\text{C}$, for all test routes, showed increased energy consumption for the Type 1 storage using LFP cells. This effect is related to the lower energy density of LFP cells, expressed in Wh/kg. While maintaining the same value of available energy (60 kWh) and a similar level of reserve (7–8%), there is an increase in vehicle weight by 476 kg compared to a vehicle with a type 2 storage (NMC cylindrical), and 496 kg compared to a vehicle with a storage type 3 (NMC pouch).

An increase in internal resistance caused by a decrease in temperature also reduces the amount of energy recovered when braking. This is visible in the data contained in Tables 6 and 7, where the smallest differences (to the detriment of lower operating temperatures), ranging from -8.38% to -10.89% , were obtained for the WLTP test route, and the largest, from -14.77% to -18.15% obtained for the actual City Flat Road route.

Based on the analysis of the results, it should be noted that the energy consumption during the tests for the selected tests is different. The highest energy consumption was demonstrated during the tests using the WLTP test for the types of energy storage, respectively 272 Wh/km, 263 Wh/km, and 249 Wh/km. The lowest energy consumption was demonstrated during tests using the City Flat Road test for energy storage types of 223 Wh/km, 222 Wh/km, and 199 Wh/km, respectively.

In addition to vehicle performance and energy consumption, each of the energy storages was analyzed in terms of predicted reliability. The reliability of each system was modeled using the reliability block diagram (RBD) methodology, assuming a serial system and one-parameter exponential distribution. The highest reliability value has energy storage Type 1 with the value of $R = 0.53$, then Type 3 with $R = 0.31$. Type 2 built

on cylindrical cells has the lowest reliability $R = 0.0000001$. The low reliability of Type 2 magazine is explained by a high number of single cells (6048) used for assembling this energy storage.

The analysis also ranks the energy storages in terms of SOH as predicted total achievable distance. The highest distance of 1,322,114 km will be achieved by vehicle with Type 1, then with Type 2 at 321,714 km, and the shortest at 273,359 by Type 2. As it is shown in Table 8, the level of charge/discharge has a significant impact on SOH. The ability to recuperate energy improves the battery life, and in the studies, the best ability has Type 1 storage, with the highest of 55.96 % recuperated energy during the City Flat Road test, but also in the ELTP-90 test with 34.31 % and WLTP test with 34.04. The worst ability for energy recuperation was Type 2 ES with 48.32 % in City Flat tests, 30.27 % in WLTP-90, and 31.34 % in WLTP.

The analysis of the test results presented in Table 9 and Figure 20, showed that the best result was obtained by the Type 1 ES (built of LFP prismatic cells) with the result $f_n(\text{Type1}) = 0.48$, the second place was the Type 3 magazine (NMC pouch) $f_n(\text{Type3}) = 0.43$ and the third Type 2 magazine (NMC cylindrical) $f_n(\text{Type2}) = 0.27$. Type 1 ES was ranked as the best choice for its cost, maximum number of cycles, reliability, lock of temperature conditioning requirements, and total range for conditions assumed in the study.

6. Conclusions

When choosing a given type of electrochemical cell chemistry, parameters such as energy density, the number of potential charging cycles to be performed, the value of the cell's internal resistance depending on the temperature, or the reliability of the energy storage structure are important elements. The conducted research has shown that the correct estimation of the above parameters can ensure the long trouble-free operation of a vehicle with an electric drive.

The proposed method of assessing the selection of cells confirmed its effectiveness. The more cells included in the energy storage, the more the risk of failure increases and the system reliability decreases. While typical damage to any of the elements (cells) of the energy storage allows continuing driving to the destination, such an event precludes further operation of the vehicle due to the BMS (Battery Management System) refusing to charge the damaged energy storage. Assuming a similar degree of reliability for each cell, whether it is a small 18650 cell or a large 160 Ah prismatic cell, the total number of component cells has a decisive impact on the durability of the critical element, which is the vehicle's energy storage.

The use of the proposed method of evaluating the parameters of electrochemical cells can bring profits to the user in the form of the trouble-free operation of a vehicle with an electric drive.

Author Contributions: Conceptualization, P.S. and A.L.; methodology, P.S. and A.L.; software, P.S. and A.L.; validation, P.S. and A.L.; formal analysis, P.S. and A.L.; investigation, P.S. and A.L.; resources, P.S. and A.L.; data curation, P.S. and A.L.; writing—original draft preparation, P.S. and A.L.; writing—review and editing, P.S. and A.L.; visualization, P.S. and A.L.; supervision, A.L.; project administration, A.L.; funding acquisition, A.L. All authors have read and agreed to the published version of the manuscript.

Funding: The project is financed within the program of the Ministry of Science and Higher Education called "Regionalna Inicjatywa Doskonałości" in the years 2019–2023, under project number 006/RID/2018/19, with a sum of financing of 11 870 000 PLN.

Conflicts of Interest: The authors declare no conflict of interest.

References

1. IEA. Sustainable Transport Development Strategy until 2030—Policies—IEA. Available online: <https://www.iea.org/policies/1226-sustainable-transport-development-strategy-until-2030> (accessed on 23 November 2022).
2. Studzieniecki, T.; Przybyłowski, A. Multilevel governance issues in EU macroregions. In Proceedings of the 6th Central European Conference in Regional Science Engines of Urban and Regional Development, Banska Bystrica, Slovakia, 20–22 September 2017.

3. Neumann, T. The Impact of Carsharing on Transport in the City. Case Study of Tri-City in Poland. *Sustainability* **2021**, *13*, 688. [CrossRef]
4. Wojciechowski, Ł.; Cisowski, T.; Małek, A. Route optimization for city cleaning vehicle. *Open Eng.* **2021**, *11*, 483–498. [CrossRef]
5. Małek, A.; Dudziak, A.; Stopka, O.; Caban, J.; Marciniak, A.; Rybicka, I. Charging Electric Vehicles from Photovoltaic Systems—Statistical Analyses of the Small Photovoltaic Farm Operation. *Energies* **2022**, *15*, 2137. [CrossRef]
6. Bartłomiej Mazan, T.D. Experimental study on the influence of temperature of lithium-ion cell on its capacity and accuracy of soc calculations. *Masz. Elektr. Zesz. Probl.* **2019**, *2*, 185–190.
7. Zhang, J.; Lee, J. A review on prognostics and health monitoring of Li-ion battery. *J. Power Source* **2011**, *196*, 6007–6014. [CrossRef]
8. Żurek-Mortka, M.; Gospodarczyk, A.; Majcher, A.; Kozak, M. Selected issues of modelling degradation of the lithium-ion batteries in electric vehicles. *Elektro Info* **2021**, *6*, 34–40, ISSN 1642-8722.
9. Śmieszek, M.; Kostian, N.; Mateichyk, V.; Mościszewski, J.; Tarandushka, L. Determination of the Model Basis for Assessing the Vehicle Energy Efficiency in Urban Traffic. *Energies* **2021**, *14*, 8538. [CrossRef]
10. Saji, D.; Babu, P.S.; Ilango, K. SoC estimation of lithium ion battery using combined coulomb counting and fuzzy logic method. In Proceedings of the 2019 4th International Conference on Recent Trends on Electronics, Information, Communication & Technology (RTEICT), Bengaluru, India, 17–18 May 2019; pp. 948–952.
11. Rudnicki, T.; Wójtowicz, S. Methods for determining the state of charge of batteries used in electric vehicles, portable devices and in the laboratory. *Inform. Autom. Pomiar Gospod. Ochr. Sr.* **2014**, *4*, 68–70. [CrossRef]
12. Chen, J.; Zhang, Y.; Wu, J.; Cheng, W.; Zhu, Q. SOC estimation for lithium-ion battery using the LSTM-RNN with extended input and constrained output. *Energy* **2023**, *262*, 125375. [CrossRef]
13. Cui, Z.; Hu, W.; Zhang, G.; Zhang, Z.; Chen, Z. An extended Kalman filter based SOC estimation method for Li-ion battery. *Energy Rep.* **2022**, *8*, 81–87. [CrossRef]
14. Hu, C.; Youn, B.D.; Chung, J. A multiscale framework with extended Kalman filter for lithium-ion battery SOC and capacity estimation. *Appl. Energy* **2012**, *92*, 694–704. [CrossRef]
15. Pang, B.; Chen, L.; Dong, Z. Data-Driven Degradation Modeling and SOH Prediction of Li-Ion Batteries. *Energies* **2022**, *15*, 5580. [CrossRef]
16. Cen, Z.; Kubiak, P. Lithium-ion battery SOC/SOH adaptive estimation via simplified single particle model. *Int. J. Energy Res.* **2020**, *44*, 12444–12459. [CrossRef]
17. Lai, X.; Yuan, M.; Tang, X.; Yao, Y.; Weng, J.; Gao, F.; Ma, W.; Zheng, Y. Co-Estimation of State-of-Charge and State-of-Health for Lithium-Ion Batteries Considering Temperature and Ageing. *Energies* **2022**, *15*, 7416. [CrossRef]
18. Babaeiyazdi, I.; Rezaei-Zare, A.; Shokrzadeh, S. State of charge prediction of EV Li-ion batteries using EIS: A machine learning approach. *Energy* **2021**, *223*, 120116. [CrossRef]
19. Kasprzyk, L. Selected issues of modeling electrochemical cells and supercapacitors in electric vehicles. *Pozn. Univ. Technol. Acad. J. Electr. Eng.* **2019**, *101*, 3–55. [CrossRef]
20. E.ON Energy Research Center. Critical Review of the Methods for Monitoring of Lithium-Ion Batteries in ... —RWTH AACHEN UNIVERSITY E.ON Energy Research Center—English. Available online: <https://www.eonerc.rwth-aachen.de/cms/E-ON-ERC/Forschung/Publicationen/~{}dmwf/Details/?file=232025&lidz=1> (accessed on 17 November 2022).
21. Wei, X.; Zhu, B.; Xu, W. Internal Resistance Identification in Vehicle Power Lithium-Ion Battery and Application in Lifetime Evaluation, Undefined. 2009. Available online: <https://www.semanticscholar.org/paper/Internal-Resistance-Identification-in-Vehicle-Power-Wei-Zhu/ed58c7472b64f7d005a90622baf1fd9be0113956> (accessed on 12 November 2022).
22. Thingvad, M.; Calearo, L.; Thingvad, A.; Viskinde, R.; Marinelli, M. Characterization of NMC Lithium-ion Battery Degradation for Improved Online State Estimation. In Proceedings of the 2020 55th International Universities Power Engineering Conference (UPEC), Torino, Italy, 1–4 September 2020; pp. 1–6.
23. Pan, H.; Lü, Z.; Wang, H.; Wei, H.; Chen, L. Novel battery state-of-health online estimation method using multiple health indicators and an extreme learning machine. *Energy* **2018**, *160*, 466–477. [CrossRef]
24. Muc, A.; Iwaszkiewicz, J.; Mysiak, P.; Piechowski, L. System zasilania falowników wielopoziomowych wykorzystujący wielopulsowe prostowniki z dławikami sprzężonymi magnetycznie. *Przegląd Elektrotechniczny* **2021**, *1*, 74–78. [CrossRef]
25. Rychlik, I. A new definition of the rainflow cycle counting method. *Int. J. Fatigue* **1987**, *9*, 119–121. [CrossRef]
26. Alternative Fuels Data Center: Batteries for Electric Vehicles. Available online: https://afdc.energy.gov/vehicles/electric_batteries.html (accessed on 10 November 2022).
27. Tomasz, R. Motor Vehicles with Electric Motor. In *Zeszyty Problemowe—Maszyny Elektryczne*; 2008; Volume 80, pp. 245–250. Available online: http://yadda.icm.edu.pl/baztech/element/bwmeta1.element.baztech-article-BPS2-0048-0091/c/ref_49_80.pdf (accessed on 14 November 2022).
28. Michalski, J.M.R. Choice of operational parameters of electric-drive cars. *Maint. Reliab.* **2008**, *3*, 69–73.
29. Energy Storage Type Serial Item No.: TSWB-LYP-Home Page | Thunder Sky Winston Battery. Available online: <https://en.winston-battery.com/?cnxcd/> (accessed on 23 November 2022).
30. Shu, X.; Yang, W.; Guo, Y.; Wei, K.; Qin, B.; Zhu, G. A reliability study of electric vehicle battery from the perspective of power supply system. *J. Power Source* **2020**, *451*, 227805. [CrossRef]
31. Batscan—Battery Reliability. Available online: <http://batscan.se/en/reliability.asp> (accessed on 16 November 2022).
32. Emission Test Cycles: WLTC. Available online: <https://dieselnet.com/standards/cycles/wltp.php> (accessed on 15 November 2022).

33. EUR-lex, Commission Regulation (EU) 2017/1151 of 1 June 2017 supplementing Regulation (EC) No 715/2007 of the European Parliament and of the Council on type-approval of motor vehicles with respect to emissions from light passenger and commercial vehicles (Euro 5 and Euro 6) and on access to vehicle repair and maintenance information, amending Directive 2007/46/EC of the European Parliament and of the Council, Commission Regulation (EC) No 692/2008 and Commission Regulation (EU) No 1230/2012 and repealing Commission Regulation (EC) No 692/2008 (Text with EEA relevance). Available online: <https://eur-lex.europa.eu/legal-content/EN/TXT/?uri=CELEX:32017R1151> (accessed on 22 November 2022).
34. The Modelica Association—Modelica Association. Available online: <https://modelica.org/> (accessed on 22 November 2022).
35. Dukalski, P.; Krok, R. Selected Aspects of Decreasing Weight of Motor Dedicated to Wheel Hub Assembly by Increasing Number of Magnetic Poles. *Energies* **2021**, *14*, 917. [CrossRef]
36. Dukalski, P.; Mikoś, J.; Krok, R. Analysis of the Simulation of the Operation of a Wheel Hub Motor Mounted in a Hybrid Drive of a Delivery Vehicle. *Energies* **2022**, *15*, 8323. [CrossRef]
37. Wiśniewski, G.; Buda, T.; Kreft, O. Application of electric drive system for electric delivery cars. *Electrotech. News* **2020**, *1*, 5–12. [CrossRef]
38. United States Environmental Protection Agency, Dynamometer Drive Schedules | US EPA. Available online: <https://www.epa.gov/vehicle-and-fuel-emissions-testing/dynamometer-drive-schedules> (accessed on 22 November 2022).
39. Yang, Y.; Lan, L.; Hao, Z.; Zhao, J.; Luo, G.; Fu, P.; Chen, Y. Life Cycle Prediction Assessment of Battery Electrical Vehicles with Special Focus on Different Lithium-Ion Power Batteries in China. *Energies* **2022**, *15*, 5321. [CrossRef]
40. Miao, Q.; Xie, L.; Cui, H.; Liang, W.; Pecht, M. Remaining useful life prediction of lithium-ion battery with unscented particle filter technique. *Microelectron. Reliab.* **2012**, *53*, 805–810. [CrossRef]
41. Abramowicz-Gerigk, T.; Burciu, Z.; Górski, W.; Reichel, M. Full scale measurements of pressure field induced on the quay wall by bow thrusters—indirect method for seabed velocities monitoring. *Ocean Eng.* **2018**, *162*, 150–160. [CrossRef]
42. Mcaleer, B. Electric Car Battery Life: Everything You Need to Know, Car and Driver. 2022. Available online: <https://www.caranddriver.com/research/a31875141/electric-car-battery-life/> (accessed on 23 November 2022).